

# Surface Chemistry and Spectroscopy of Chromium in Inorganic Oxides

Bert M. Weckhuysen,<sup>\*,†</sup> Israel E. Wachs,<sup>‡</sup> and Robert A. Schoonheydt<sup>†</sup>

Centrum voor Oppervlaktechemie en Katalyse, Katholieke Universiteit Leuven, Kardinaal Mercierlaan 92, 3001 Heverlee, Belgium and Zettlemoyer Center for Surface Studies, Departments of Chemistry and Chemical Engineering, Lehigh University, Bethlehem, Pennsylvania 18015

Received July 31, 1995 (Revised Manuscript Received May 8, 1996)

## Contents

I. Introduction	3327
A. General Introduction	3327
B. Scope of the Review	3328
II. Molecular Structure of Cr in Aqueous Media and in the Solid State	3328
A. Molecular Structure of Cr in Aqueous Media	3329
B. Molecular Structure of Cr in the Solid State	3329
III. Characterization Methods	3330
IV. Molecular Structure of Cr on Oxidic Surfaces	3331
A. Molecular Structure of Cr on Amorphous Oxides	3331
1. Hydrated Cr	3331
2. Anchored Cr	3332
3. Reduced Cr	3334
B. Molecular Structure of Cr on Molecular Sieves	3335
1. Chromium Ion-Exchanged and -Impregnated Molecular Sieves	3335
2. Hydrothermally Synthesized, Chromium-Containing Molecular Sieves	3338
V. Quantitation of Cr Species on Oxidic Surfaces	3339
VI. Mobility and Surface Reactivity of Cr on Oxidic Surfaces	3339
A. Mobility of Supported Cr	3339
B. Surface Reactivity of Supported Cr	3343
VII. Catalysis of Cr on Oxidic Surfaces	3344
A. Oxidation Reactions	3344
B. Hydrogenation–Dehydrogenation Reactions	3345
C. Polymerization Reactions	3346
VIII. Concluding Remarks	3346
IX. List of Abbreviations	3347
X. Acknowledgments	3347
XI. References	3347

## I. Introduction

### A. General Introduction

Among the transition metal ions of the 3d series, Cr takes a particular position because of its variability in oxidation state, coordination numbers and molecular structure.<sup>1,2</sup> The elucidation of these Cr species on inorganic oxidic surfaces is a complex task, which is of fundamental importance to understanding the behavior of Cr in the environment, colloids, and Cr-based heterogeneous catalysts.<sup>3–6</sup>

The environmental behavior of Cr is illustrated in Figure 1. Chromium is frequently encountered in

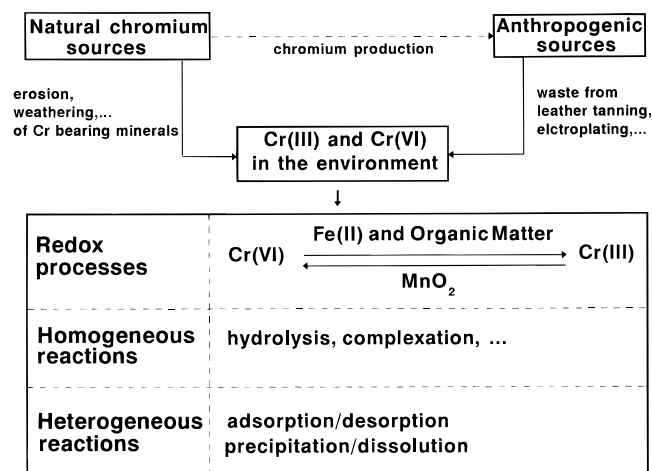


**Figure 1.** Behavior of Cr in the environment. Chromium ions can be released from natural chromium sources or by man in the environment, where it is susceptible to redox and homogeneous and/or heterogeneous reactions.

minerals and in geochemical deposits,<sup>7</sup> and due to erosion and weathering, chromium becomes a surface species or can be released into the environment. On the other hand, Cr compounds are used in industries such as leather tanning, electroplating, and pigment production and, therefore, are found in solid wastes and in waste waters. All these Cr oxides are highly soluble and susceptible to various reactions at the solid–water interface: redox processes and homogeneous and heterogeneous reactions. Chromium might be oxidized or reduced by soil constituents and such redox reactions have dramatic influences on the behavior of Cr.<sup>8,9</sup> The water soluble and mobile Cr<sup>6+</sup> is toxic, while the hazard of the less mobile Cr<sup>3+</sup> is relatively low. Manganese oxides are the known naturally occurring oxidants of Cr<sup>3+</sup>, while Cr<sup>6+</sup> is reduced to the less mobile Cr<sup>3+</sup> by organic soil constituents (amino, humic, and fulvic acids) and Fe<sup>2+</sup>.

Chromium-based catalysts are composed of Cr oxides supported on inorganic oxides, such as silica, alumina, and molecular sieves. Chromium on silica (Cr/SiO<sub>2</sub>), as illustrated in Figure 2, is the famous Phillips catalyst for the polymerization of ethylene at relatively low pressures.<sup>10–13</sup> This catalyst is the basis for the Phillips particle form process in the production of high-density polyethylene (HDPE), one of the most extensively used polymers. Other important catalytic activities are hydrogenation–dehydrogenation, oxidation, isomerization, aromatization, and DeNO<sub>x</sub> reactions.<sup>14–28</sup> The basis for the activity of Cr in such a wide spectrum of reactions lies in the variability of oxidation states, of coordination envi-

\* Author to whom correspondence should be addressed.

<sup>†</sup> Katholieke Universiteit Leuven.

<sup>‡</sup> Lehigh University.



Bert M. Weckhuysen was born on July 27, 1968, in Aarschot, Belgium. In 1991 he received his M.S. degree from the Faculty of Agronomy and Applied Biological Sciences, Catholic University of Leuven, Belgium. From 1991 to 1995 he was employed as a doctoral student at the Center for Surface Chemistry and Catalysis of the same faculty under the supervision of Professor Robert A. Schoonheydt. There he gained experience in spectroscopic techniques, zeolite synthesis, catalyst design, and characterization. After obtaining his Ph.D. in Applied Biological Sciences from the Department of Interphase Chemistry in 1995, he has worked as a visiting research scientist with Professor Israel E. Wachs at the Zettlemoyer Center for Surface Studies of Lehigh University. Presently, he is a postdoctoral research fellow of the National Fund of Scientific Research at the Catholic University of Leuven and a postdoctoral research associate at the Chemistry Department of Texas A & M University.

ronments, and of degree of polymerization of Cr oxide species. This variability is especially pronounced on the surface. Thus, knowledge about the surface chemistry of Cr in inorganic oxides is of key importance in environmental sciences and heterogeneous catalysis.

## B. Scope of the Review

A prerequisite for understanding the behavior of Cr on surfaces of inorganic oxides is a thorough knowledge of the chemistry and its dependence on the type and composition of the inorganic oxide as well as environmental conditions. In this review, fundamental advances into the surface chemistry and spectroscopy of Cr in inorganic oxides since 1985, the publication year of the review of McDaniel,<sup>6</sup> are emphasized. We will restrict ourself to amorphous supports and molecular sieves and, thus, oxygen is the main ligand of Cr.



Robert A. Schoonheydt received his M.S. degree in 1966 and his Ph.D. in 1970, both under the supervision of Professor Jan B. Uytterhoeven at the Catholic University of Leuven, Belgium. After one year as a postdoc with Professor Jack H. Lunsford in the Chemistry Department of Texas A&M University, he returned to the Catholic University of Leuven as a National Fund of Scientific Research researcher. He became full professor at the same institute in 1989. His teaching responsibilities include physical and analytical chemistry for engineering students at the Faculty of Agronomy and Applied Biological Sciences. His research is concentrated in three areas: (1) spectroscopy and chemistry of surface transition metal ions; (2) molecular organization on clay surfaces; and (3) theoretical modeling of molecule–surface interactions. Presently, he is secretary-general of AIPEA and head of the Department of Interphase Chemistry.

With the basic principles of solution and solid-state chromium chemistry as the starting point, it will be shown that (1) the support type and composition play a decisive role in the speciation of Cr; (2) a battery of complementary techniques (DRS, RS, IR, XPS, TPR, ESR, EXAFS-XANES, etc.) is necessary to unravel the surface chemistry of Cr; (3) the oxidation states of Cr can be spectroscopically quantified in well-defined conditions; and (4) surface Cr ions are mobile and possess catalytic activity.

## II. Molecular Structure of Cr in Aqueous Media and in the Solid State

Chromium occurs with different coordination numbers (2, 3, 4, 5, and 6), different oxidation states ( $\text{Cr}^{n+}$  with  $n = 2, 3, 4, 5,$  and  $6$ ), and molecular structures (chromate, dichromate, trichromate, etc.).<sup>1</sup>  $\text{Cr}^{6+}$  ( $d^0$ ) ions are the mostly tetrahedrally coordinated and tend to form polyoxoanions.  $\text{Cr}^{3+}$  ( $d^3$ ) is the most stable oxidation state and has been extensively

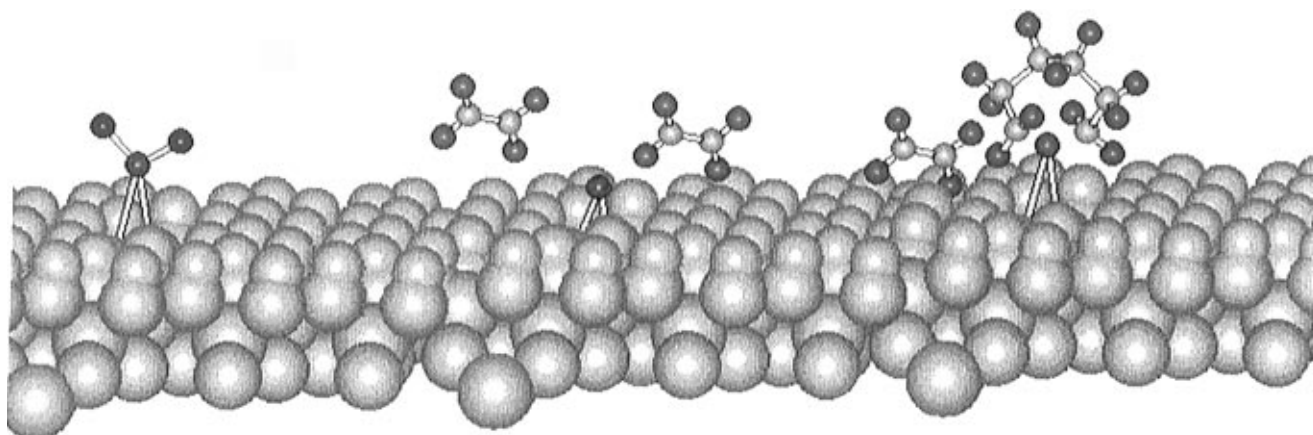


**Figure 2.** Pictorial representation of a Phillips Polymerization Catalyst ( $\text{Cr}/\text{SiO}_2$ ). Interaction between ethylene molecules and supported Cr and oligomerization of ethylene. [Space-filling molecular model (as generated by Hyperchem): green, chromium; blue, oxygen; yellow, carbon; red, hydrogen; and gray, oxidic support].



Israel E. Wachs received his B.E. degree in Chemical Engineering from The City College of The City University of New York in 1973. He received his M.S. degree in 1974 and his Ph.D. in Chemical Engineering in 1977 from Stanford University under the supervision of Professor R. J. Madix. He joined the Corporate Research Laboratories of Exxon Research & Engineering Co. in 1977 where he was involved in fundamental and applied research in the areas of selective oxidation, hydrocarbon conversion, hydrogenation of carbon monoxide (Fisher-Tropsch synthesis), and hydrodesulfurization catalysis. In 1987, he became an Associate Professor of Chemical Engineering at Lehigh University and was promoted to full Professor in 1992. His teaching responsibilities include heterogeneous catalysis and surface characterization, fundamentals of air pollution, advanced technologies in chemical engineering, chemical reaction engineering, unit operations and fluid mechanics. His research program has focused on the synthesis, characterization, and catalysis of supported metal oxide catalysts with special emphasis on the molecular structure–reactivity relationships of oxidation reactions. He is the editor of the book *Characterization of Catalytic Materials* (Butterworths-Heinemann, 1992).

studied. The oxidation states of  $\text{Cr}^{5+}$  ( $d^1$ ) and  $\text{Cr}^{4+}$  ( $d^2$ ) are rather unstable and  $\text{Cr}^{5+}$  easily disproportionates to  $\text{Cr}^{3+}$  and  $\text{Cr}^{6+}$ . The  $\text{Cr}^{2+}$  ( $d^4$ ) ions are strongly reducing and only stable in the absence of oxygen.

### A. Molecular Structure of Cr in Aqueous Media

The most important oxidation states in solution are  $\text{Cr}^{6+}$ ,  $\text{Cr}^{3+}$ , and  $\text{Cr}^{2+}$ .<sup>1</sup> The specific chromium oxide species that can exist depend on the solution pH, the chromium oxide concentration, and the redox potential.  $\text{Cr}^{6+}$ , for example, may be present in water as chromate ( $\text{CrO}_4^{2-}$ ), dichromate ( $\text{Cr}_2\text{O}_7^{2-}$ ), hydrogen chromate ( $\text{HCrO}_4^-$ ), dihydrogen chromate ( $\text{H}_2\text{CrO}_4$ ), hydrogen dichromate ( $\text{HCr}_2\text{O}_7^{2-}$ ), trichromate ( $\text{Cr}_3\text{O}_{10}^{2-}$ ), and tetrachromate ( $\text{Cr}_4\text{O}_{13}^{2-}$ ). The last three ions have been detected only in solutions of  $\text{pH} < 0$  or at chromium(VI) concentrations greater than 1 M. Polyanions containing more than four chromium atoms are not known in solution.

All these features can be understood on the basis of the Pourbaix diagram presented in Figure 3.<sup>29</sup> Above  $\text{pH} 8$ , only  $\text{CrO}_4^{2-}$  is stable, and as the  $\text{pH}$  decreases into the  $\text{pH}$  region 2–6, the equilibria shifts to dichromate according to the overall equilibrium:



At still lower  $\text{pH}$  values and concentrated media, tri- and tetrachromates are formed (respectively  $\text{Cr}_3\text{O}_{10}^{2-}$  and  $\text{Cr}_4\text{O}_{13}^{2-}$ ). In summary, decreasing of the  $\text{pH}$  or increasing the chromium oxide concentration results in the formation of more polymerized chromium oxide species. The  $\text{Cr}^{6+}$  species is a strong

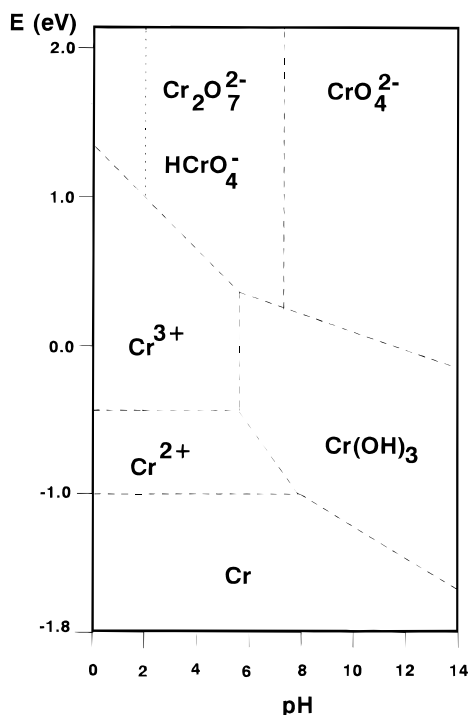
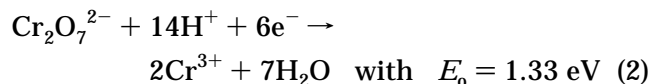
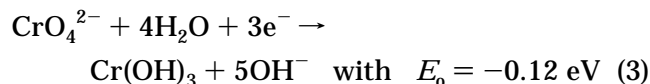


**Figure 3.** The Pourbaix diagram of chromium, expressing the Cr speciation as a function of  $\text{pH}$  and potential ( $T = 25^\circ\text{C}$ ) (Redrawn from ref 29).

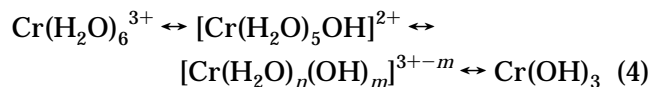
oxidant but the redox potential depends on the  $\text{pH}$ . In acidic media, the following reaction is involved



while in basic solution



In acid solution,  $\text{Cr}^{3+}$  is always an octahedral hexaquo ion,  $\text{Cr}(\text{H}_2\text{O})_6^{3+}$ . It tends to hydrolyze with increasing  $\text{pH}$ , resulting in the formation of polynuclear complexes containing  $\text{OH}^-$  bridges.<sup>30</sup> This is thought to occur by the loss of a proton from coordinated water, followed by coordination of the  $\text{OH}^-$  to a second cation. The final product of this hydrolysis is hydrated chromium(III) oxide or chromic hydroxide ( $\text{Cr}(\text{OH})_3$ ). The following equilibria are thus observed with increasing  $\text{pH}$ :



The aqueous chemistry of the strongly reducing  $\text{Cr}^{2+}$  cation has not been as extensively studied because of its instability.  $\text{Cr}^{2+}$  ions are present in water as octahedral high-spin hexaquo ions,  $\text{Cr}(\text{H}_2\text{O})_6^{2+}$ , and are unstable with respect to oxidation to  $\text{Cr}^{3+}$ :



### B. Molecular Structure of Cr in the Solid State

The principal chromium oxides are  $\text{CrO}_3$ ,  $\text{CrO}_2$ , and  $\text{Cr}_2\text{O}_3$ , but some intermediate states, like  $\text{Cr}_3\text{O}_8$ ,

**Table 1. Characterization Techniques for Cr Speciation and the Obtained Information on Coordination, Oxidation States, and Dispersion**

technique	oxidation state					coordination	dispersion	quantitative	minimum detectable amount (wt % Cr)
	6	5	4	3	2				
DRS	+	-	-	+	+	+	-	+	<0.1
ESR	-	+	-	+	-	+	±	+	<0.1
IR	+	-	-	+	+	+	-	-	<0.2
RS	+	-	-	+	+	+	+	-	<0.2
XPS	+	+	-	+	+	-	+	+	>0.4
EXAFS-XANES	±	±	±	±	±	+	-	-	>2.0
TPO-TPR	-	±	±	±	±	-	+	+	>0.8
SQUID	-	+	+	+	+	-	-	+	<0.1
SIMS	-	-	-	-	-	±	±	-	>1
XRD	-	-	-	-	-	+	±	-	>5
ISS	-	-	-	-	-	-	+	-	-
CO <sub>2</sub> -chemisorption	-	-	-	-	-	-	+	-	-

**Table 2. Spectroscopic Fingerprints of Supported Cr Species**

spectroscopic technique	spectroscopic signature	type of signature	Cr species	ref(s)
ESR	axially symmetric/rhombic signal with $g$ around 2 and $ppw < 60$ G		isolated Cr <sup>5+</sup> ( $\gamma$ -signal)	34-47
	nearly isotropic and broad signal ( $g = 1.9-2.4$ ) with $40 < ppw < 1800$ G		Cr <sub>2</sub> O <sub>3</sub> -like clusters ( $\beta$ -signal)/ Cr(H <sub>2</sub> O) <sub>6</sub> <sup>3+</sup> complexes	
DRS	broad signal around $g = 4$ with high $D$ and $E$ values		isolated Cr <sup>3+</sup> in highly distorted octahedral coordination ( $\delta$ -signal)	
	27000-30000; 36000-41000 cm <sup>-1</sup>	charge transfers	chromate	48-58
	21000-23000; 27000-30000; 36000-41000 cm <sup>-1</sup>	d-d transitions	polychromate	
RS	15000-17000 cm <sup>-1</sup>		(pseudo-) octahedral Cr <sup>3+</sup> , including Cr <sub>2</sub> O <sub>3</sub>	
	10000-13000 cm <sup>-1</sup>		(pseudo-) octahedral Cr <sup>2+</sup>	
	7000-10000 cm <sup>-1</sup>		(pseudo-) tetrahedral Cr <sup>2+</sup>	
	865 cm <sup>-1</sup>	Cr-O vibrations	hydrated chromate	59-68
	900; 942 cm <sup>-1</sup>		hydrated dichromate	
IR	904; 956; 987 cm <sup>-1</sup>		hydrated trichromate	
	980-990 cm <sup>-1</sup>		dehydrated monochromate	
	1000-1010; 850-880 cm <sup>-1</sup>		dehydrated polychromate	
	550 cm <sup>-1</sup>		octahedral Cr <sup>3+</sup>	
	900-950 cm <sup>-1</sup> (1800-1900 cm <sup>-1</sup> in first overtone)	Cr-O vibrations	Cr <sup>6+</sup>	64,69-85
XPS	2178; 2184 cm <sup>-1</sup>	CO vibrations	Cr <sup>2+</sup> with CN = 2 before chemisorption (CrA species)	
	2191 cm <sup>-1</sup>		Cr <sup>2+</sup> with CN = 3 before chemisorption (CrB species)	
	no chemisorption		Cr <sup>2+</sup> with CN = 4 before chemisorption (CrC species)	
	580 eV		Cr <sup>6+</sup>	86-91
			Cr <sup>5+</sup>	
			Cr <sup>3+</sup>	
			Cr <sup>2+</sup>	

Cr<sub>2</sub>O<sub>5</sub>, and Cr<sub>5</sub>O<sub>12</sub>, have also been observed.<sup>31,32</sup> The red orthorhombic chromium trioxide (CrO<sub>3</sub>) crystals are made up of chains of corner-shared CrO<sub>4</sub> tetrahedra. They lose oxygen upon heating to give a succession of lower oxides until the green Cr<sub>2</sub>O<sub>3</sub> is formed. The latter oxide is the most stable oxide and has a spinel structure. The third major oxide of chromium is the brown-black, CrO<sub>2</sub>, which is an intermediate product in the decomposition of CrO<sub>3</sub> to Cr<sub>2</sub>O<sub>3</sub> and possesses a rutile structure.

Chromium is also frequently encountered in minerals and these Cr-bearing minerals contain either hexa-, tri- or divalent Cr.<sup>33</sup> The most common minerals contain (distorted) octahedral Cr<sup>3+</sup> (e.g. chromite, ruby, muscovites and tourmaline), which gives most of these minerals a green color. Although Cr<sup>2+</sup> ions are rare and unstable in terrestrial minerals, their presence is suspected in the blue minerals olivine and pyroxene. Cr<sup>2+</sup> ions are frequently octa-

hedrally coordinated, but tetrahedral Cr<sup>2+</sup> exists in spinel-like minerals.

### III. Characterization Methods

The characterization of the molecular structure of supported chromium ions is rather involved, since deposition of this metal ion on a support can result in (1) isolated chromium ions, (2) a two-dimensional chromium oxide overlayer, or (3) three-dimensional chromium oxide crystallites. Moreover, each phase can simultaneously possess several different molecular structures. Thus, useful characterization techniques, which can provide detailed information about the molecular structure of the supported chromium oxide, must be capable of discriminating between these different states and of quantifying the individual oxidation states. The spectra are complex and usually encompasses several overlapping bands, so that band decomposition routines and chemometrical

techniques need to be employed. This is especially important if quantitative information is desired.

The different techniques used in the literature for studying supported Cr are summarized in Table 1 (list of abbreviations provided at end of the paper), together with the obtained information about speciation, dispersions and coordination. The given information about speciation concerns only the detectable oxidation states, while dispersion can be defined as the ratio of the amount of Cr probed by a particular characterization technique over the total amount present on the surface. Furthermore, the minimum detectable amounts are the minimum values reported in the literature. It is also important to state that the different characterization techniques are only quantitative under well-defined conditions. In the case of ESR, problems with quantification may arise if spin-spin interactions or fast relaxation processes occur. The binding energies (BE), measured by XPS, increases with increasing oxidation state and for a fixed oxidation state with the electronegativity of the surrounding atoms. The BE values are also influenced by the degree of dispersion and bulk chromium oxides always exhibit lower BE values compared to Cr ions dispersed in inorganic oxides. As a result, the estimation of the valence states only from BE values is very difficult. In addition, highly dispersed Cr<sup>6+</sup> and Cr<sup>5+</sup> are readily reduced under high vacuum in the ESCA chamber and/or under influence of X-ray irradiation, and consequently complicating the estimation of the different oxidation states from XPS data.<sup>86,87</sup>

The five most applied spectroscopic characterization tools are ESR, DRS, RS, IR, and XPS, and their spectroscopic fingerprints of the observed Cr species are given in Table 2.<sup>34-91</sup> It is clear that no characterization technique will be capable of providing all the information needed for complete characterization. Thus, successful characterization of chromium in inorganic oxides requires a multitechnique approach.

#### IV. Molecular Structure of Cr on Oxidic Surfaces

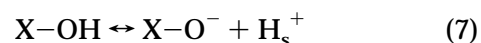
##### A. Molecular Structure of Cr on Amorphous Oxides

The molecular structure of Cr on amorphous oxides is strongly dependent on the environmental conditions (hydrated, dehydrated, oxidized, and reduced environments) and on the type and composition of the support (SiO<sub>2</sub>, Al<sub>2</sub>O<sub>3</sub>, SiO<sub>2</sub>·Al<sub>2</sub>O<sub>3</sub>, MgO, ZrO<sub>2</sub>, TiO<sub>2</sub>, AlPO<sub>4</sub>, Nb<sub>2</sub>O<sub>5</sub>, and SnO<sub>2</sub>).

###### 1. Hydrated Cr

Under hydrated conditions, the surface of an amorphous oxide is covered by a thin water film and

its hydroxyl population is subject to pH-dependent equilibria reactions:<sup>3,4,92</sup>



with X = Si, Al, Ti, Mg, Nb, Sn or Zr; H<sub>s</sub><sup>+</sup> and H<sup>+</sup> represent the surface and solution proton, respectively; K<sub>1</sub> = ([X-OH]\*[H<sub>s</sub><sup>+</sup>])/[X-OH<sub>2</sub><sup>+</sup>]; K<sub>2</sub> = ([X-O<sup>-</sup>]\*[H<sub>s</sub><sup>+</sup>])/[X-OH] and the isoelectric point (IEP) = (pK<sub>1</sub> + pK<sub>2</sub>)/2 and represents the pH at which the surface of the oxide has a net zero charge. The IEP's are dependent on oxide type and composition as shown in Table 3. The lower the IEP of the amorphous oxide, the more the equilibria of the reactions 6-8 are driven to the right. The higher the H<sup>+</sup> concentration near the surface, the more the equilibria of reactions 1 and 4 are driven toward the formation of dichromate and a Cr(H<sub>2</sub>O)<sub>6</sub><sup>3+</sup> complex, respectively.

Spectroscopic measurements on supports with low Cr<sup>6+</sup> loadings, confirm these findings, and the obtained speciation is summarized in Table 3. DRS experiments show that the monochromate:dichromate ratio decreases with increasing Si:Al ratio of silica aluminas, while by Raman spectroscopy, monochromate is observed on MgO, Al<sub>2</sub>O<sub>3</sub>, ZrO<sub>2</sub>, and TiO<sub>2</sub> and mainly polychromates (dichromate, etc.) on SiO<sub>2</sub>. As an example, Figure 4 shows the DRS and RS spectra of hydrated Cr/Al<sub>2</sub>O<sub>3</sub> catalysts as a function of the Cr loading. Instead, Cr<sup>3+</sup> species are difficult to discriminate on hydrated surfaces by spectroscopy and the different species of eq 4 cannot be clearly distinguished. In any case, the broad isotropic ESR signal around g = 2 and the typical DRS absorptions at around 17 000 and 23 000 cm<sup>-1</sup> are indicative for the presence of hydrated octahedral Cr<sup>3+</sup> complexes.

When the Cr loading (as e.g. CrO<sub>3</sub>) increases two effects come into play: (1) the pH near the surface is lowered due to presence of chromium and decreases with increasing Cr loading and (2) the dispersion depends on the available surface area as well as availability of reactive surface hydroxyl groups. Both factors influence the chemistry of chromium in the same direction, i.e. toward the formation of surface polychromates. The detected Cr<sup>6+</sup> species are described in Table 3, while Figure 5 illustrates the speciation of hydrated Cr on surfaces of amorphous supports. It is also important to stress that the presence of anions and cations (Na<sup>+</sup>, F<sup>-</sup>, etc.) on the

**Table 3. Observed Surface Chromium Oxide Species on Different Hydrated Amorphous Inorganic Oxides**

oxide	IEP	Cr oxide at low Cr loading	Cr oxide at high Cr loading	ref(s)
MgO	11.0	chromate	chromate	68
Al <sub>2</sub> O <sub>3</sub>	8.9	chromate	chromate and dichromate	56,57,63,66,68,94
TiO <sub>2</sub>	6.2	chromate	chromate and dichromate	68
ZrO <sub>2</sub>	5.9	chromate	dichromate and chromate	68
SiO <sub>2</sub> ·Al <sub>2</sub> O <sub>3</sub>	4.5	chromate and some dichromate	dichromate and chromate	68,93
Nb <sub>2</sub> O <sub>5</sub>	4.2	chromate and some dichromate	dichromate and chromate	95
SiO <sub>2</sub>	3.9	chromate and some dichromate	trichromate, dichromate and chromate	68,94
SiO <sub>2</sub>	2.0	dichromate and some chromate	tetrachromate, trichromate, dichromate	56,57,93

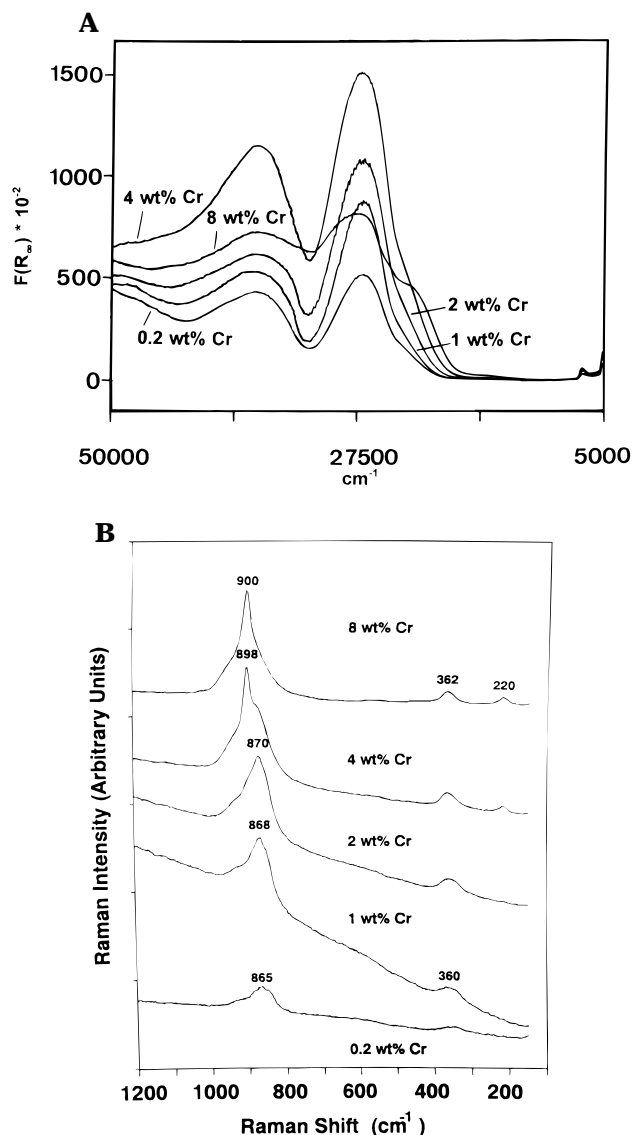


**Figure 4.** DRS (A) and RS (B) spectra of hydrated Cr on an alumina surface for increasing Cr loading (Reprinted from ref 93. Copyright 1995 Royal Chemical Society.)

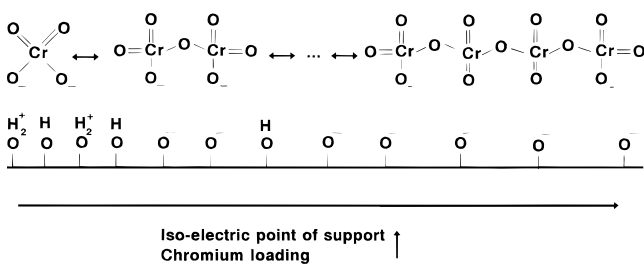


**Figure 5.** Surface chemistry of hydrated Cr on amorphous surfaces, showing the relation between the polymerization degree of Cr on the one hand and the isoelectric point of the support and the Cr loading on the other hand (redrawn from ref 106).

surfaces can alter the isoelectric point of the supports and, consequently, the Cr speciation.

## 2. Anchored Cr

Upon heating in air, the water molecules adsorbed on the support and around Cr are removed, while  $\text{Cr}^{3+}$  ions (if present) are oxidized to  $\text{Cr}^{6+}$ . The formed dehydrated chromium oxide species do not decompose into  $\text{O}_2$  and  $\text{Cr}_2\text{O}_3$  (like the pure compounds), at least for low Cr loadings, but are an-

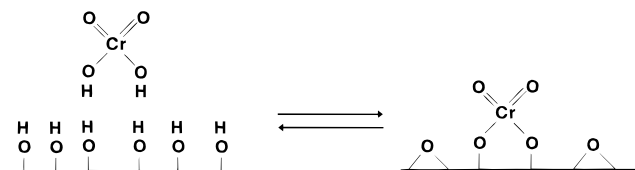


**Figure 6.** Anchoring reaction of chromate on an alumina support. Reaction of Cr with the hydroxyl groups and dehydroxylation process of the surface oxide (redrawn from ref 106).

chored by an esterification reaction with the hydroxyl groups of the inorganic oxide, resulting in the formation of surface Cr species. This is schematically drawn for Cr on alumina in Figure 6. Evidence for this anchorage reaction comes from the following:

(1) Infrared spectroscopy<sup>47,78,65</sup> and diffuse reflectance spectroscopy in the near-infrared region,<sup>93</sup> indicating the consumption of OH groups. This OH consumption is proportional to the quantity of deposited Cr, and Turek *et al.*<sup>96</sup> have shown that on alumina this OH consumption starts from the more basic OH groups to the more acidic groups.

(2) Experiments with  $\text{CrO}_2\text{Cl}_2$  and silica, which show the release of HCl and the reverse reaction of dry HCl with calcined  $\text{Cr/SiO}_2$  with release of  $\text{CrO}_2\text{Cl}_2$  vapor.<sup>97–100</sup>

(3) The exothermal peak in DTA curves around 250 °C, which is ascribed to this esterification reaction.<sup>101</sup>

This anchorage process can be envisaged as an acid–base reaction because the weaker acid  $\text{H}_2\text{O}$  is replaced by the stronger one  $\text{H}_2\text{CrO}_4$ . The reaction is therefore most pronounced on the more basic alumina. Furthermore, the most basic OH groups react preferentially, while the less basic OH groups only react at higher Cr loadings. Silica surfaces contain more acidic hydroxyl groups and have, therefore, a poor capacity for Cr anchoring. Consequently,  $\text{Cr}_2\text{O}_3$  particles are frequently encountered on silica surfaces, even at very low Cr loadings.<sup>56–57</sup>

The molecular structure of the anchored  $\text{Cr}^{6+}$  is a strong point of discussion in the literature,<sup>6</sup> and several molecular structures, starting from monochromate over dichromate to polychromate, are proposed. Many researchers have measured the change in hydroxyl population of a silica surface on anchoring of chromium: a monochromate species should react with two hydroxyls per Cr, while dichromate displaces only one per Cr. However, the results from this approach were extremely contradictory. Hogan<sup>11</sup> and McDaniel<sup>97–100</sup> concluded that  $\text{CrO}_3$  attaches mainly as monochromate, while Zecchina *et al.*<sup>48</sup> and Krauss<sup>52</sup> reported that dichromate was the dominant species. Others have tried to correlate the geometry of chromate and dichromate with models of amorphous supports.<sup>6</sup> Although they show that dichromate is favored on silica, these kind of studies are too uncertain due to the lack of information about silica surfaces and the surfaces of amorphous supports in general. Furthermore, the oxide surfaces may become restructured upon the anchoring of Cr.

Direct information about the molecular structure can be found by the application of different spectroscopic techniques such as diffuse reflectance spectroscopy, Raman spectroscopy, infrared spectroscopy, and X-ray absorption spectroscopy. The molecular structures of a series of anchored chromium oxide

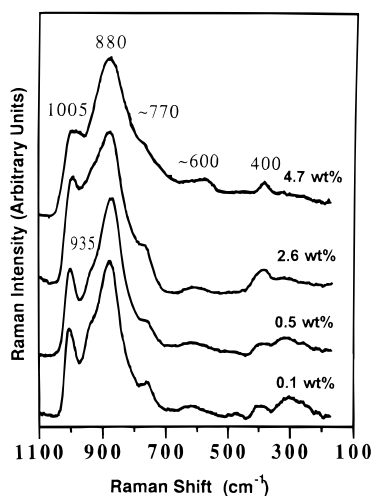


**Figure 7.** RS spectra of calcined  $\text{Cr}/\text{Al}_2\text{O}_3$  catalysts for increasing Cr loading. (Reprinted from ref 64. Copyright 1992 American Chemical Society).

catalysts on silica, alumina, titania, zirconia, niobia, and magnesia were systematically investigated with Raman, IR, and DRS after dehydration at 450–550 °C.<sup>62,64,65,94</sup> For  $\text{Cr}/\text{SiO}_2$  (Cab-O-Sil, 300  $\text{m}^2/\text{g}$ ), the dominant surface chromium oxide species detected by Raman and DRS was monochromate, but amounts of polychromate were also detected by DRS to be present at higher Cr loadings. However, for surface chromium oxide on alumina (Harshaw, 180  $\text{m}^2/\text{g}$ ), the polychromate species was the major species detected by Raman and DRS, especially at high Cr loadings. This is illustrated in Figure 7 by some RS spectra of dehydrated  $\text{Cr}/\text{Al}_2\text{O}_3$  catalysts with increasing Cr loading. Anchored chromium oxide species on titania (Degussa P-25, 55  $\text{m}^2/\text{g}$ ), zirconia (Degussa, 39  $\text{m}^2/\text{g}$ ), and niobia (Niobium Products Co., 37  $\text{m}^2/\text{g}$ ) were predominantly present as polychromate species and gave similar Raman and IR vibrations to those observed for  $\text{Cr}/\text{Al}_2\text{O}_3$ . There is a general agreement that the surface monochromate species on silica possesses a dioxo structure, but there is still some uncertainty as to whether the surface polychromate species on the other oxide supports possesses a monooxo or dioxo structure.<sup>64</sup> Hopefully, this issue can be resolved in the near future with oxygen isotope experiments. For  $\text{Cr}/\text{MgO}$  (Fluka Chemical Co., 80  $\text{m}^2/\text{g}$ ), a solid solution is formed, rather than a surface chromium oxide species, due to the strong acid–base reaction between the acidic chromia and the strongly basic magnesia.<sup>61</sup> Thus, the molecular structure of the surface chromium oxide species is strongly dependent on the surface properties of the oxide support, i.e. the surface hydroxyl chemistry and the available surface area.

The ratio of surface monochromate to polychromate species can be altered by changing the surface chemistry of the oxide surfaces. For example, the addition of submonolayer quantities of surface titania species to silica (Cab-O-Sil) enhances the concentration of surface polychromate species and results in comparable amounts of surface monochromate and polychromate species.<sup>67</sup> The formation of a surface silica overlayer on titania (Degussa P-25) suppresses the concentration of surface polychromate species and increases the amounts of surface monochromate species.<sup>66</sup> In addition, the surface chromium oxide

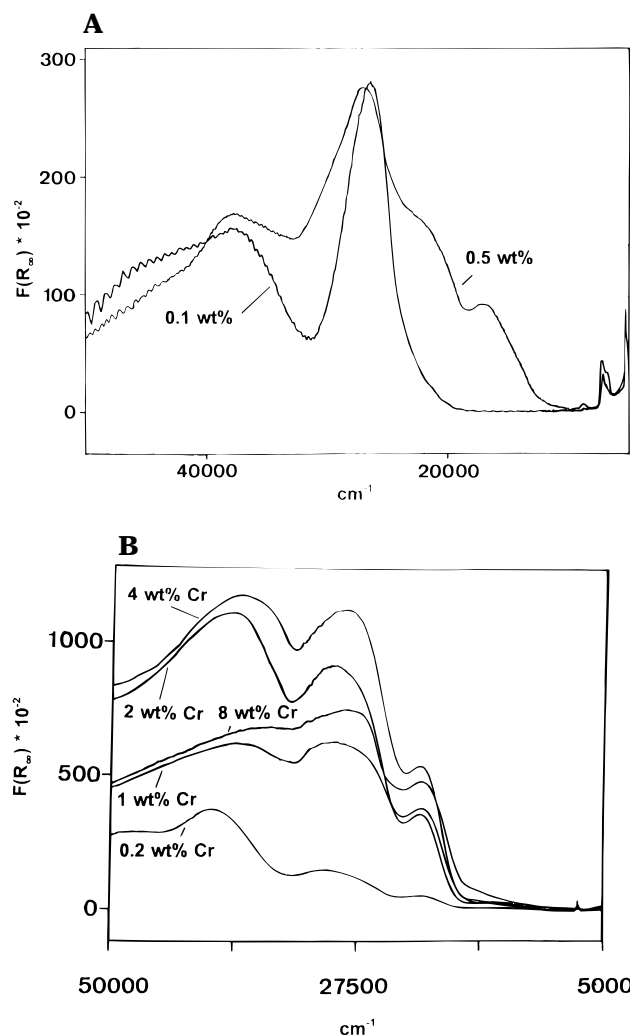


**Figure 8.** DRS spectra of calcined  $\text{Cr}/\text{SiO}_2$  catalysts for increasing Cr loading. (A) Industrially prepared pyrogenic silica and (B) sol-gel method based silica. (Part A: redrawn from ref 94. (Part B: Reprinted from ref 93. Copyright 1995 Royal Chemical Society.)

species is also sensitive to the support type and more particularly to the specific preparation method. This is illustrated in the DRS spectra of Figure 8 which reveals that surface monochromate species is the dominant species on industrial pyrogenic silica (Cab-O-Sil, 300  $\text{m}^2/\text{g}$ ) and that surface polychromate species is the dominant species on laboratory sol-gel silica (700  $\text{m}^2/\text{g}$ ). The ratio of surface polychromate to monochromate species can also be varied for the sol-gel supports by altering the Si:Al ratio and increases with increasing Si:Al ratio and Cr loading. Thus, on alumina mainly monochromate is formed, although at high Cr loadings (around 8 wt % Cr) dichromates are formed; while on silica surfaces, polychromates dominate over monochromates. Consequently, the molecular structure of Cr not only depends on the Cr loading, the support composition, but also on the surface chemistry of the oxide support which may be further modified by the preparation and calcination procedures. These dependencies explain why the data in the literature are sometimes difficult to compare and only by a combination of different spectroscopic techniques can detailed molecular-level information be obtained. In light of our current understanding, it is not surprising there has been such confusion for the last 30 years on the

molecular structure of supported Cr on dehydrated surfaces.<sup>6</sup>

In addition to the chromates, Cr<sup>5+</sup> ions and Cr<sub>2</sub>O<sub>3</sub> clusters can also be formed on calcined surfaces and their relative amount is support, loading, and treatment dependent. The Cr<sup>5+</sup> ions are easily detectable by ESR as the  $\gamma$  signal. Although this  $\gamma$  signal is generally attributed to Cr<sup>5+</sup> in square-pyramidal or distorted tetrahedral coordination,<sup>34–37</sup> some researchers insist that it involves a combination of Cr<sup>6+</sup> and Cr<sup>3+</sup> (i.e. a Zener double exchange system).<sup>102–104</sup> Detailed ESR studies of Cr<sup>45-</sup> and of Cr<sup>53-</sup>-enriched supported Cr systems,<sup>36,105,46</sup> and SQUID measurements<sup>106</sup> reject this hypothesis and show that Cr<sup>5+</sup> is present as an isolated paramagnetic ion, following the Curie–Weiss law down to 10 K. Only between 10 and 4.5 K were antiferromagnetic features observed and consequently the Curie–Weiss plot deviates from linearity.<sup>106</sup>

Cr<sub>2</sub>O<sub>3</sub> formation can be studied by DRS, ESR, RS, and XRD and is the most pronounced on silica-rich supports with a high Cr loading and after heating at high temperature with a high heating rate. Thus, as the chromium loading increases, almost all is stabilized in the hexavalent state until a certain saturation coverage is reached, because Cr titrates the surface hydroxyls, which depends on the calcination procedure.<sup>98–100</sup> Beyond this limit, excess Cr is converted to Cr<sub>2</sub>O<sub>3</sub>. Finally, techniques like N<sub>2</sub> adsorption and XPS are used to determine the dispersion of Cr. Fouad *et al.* showed by N<sub>2</sub> adsorption measurements that the dispersion of Cr is the lowest on silica and the highest on alumina surfaces.<sup>107</sup> In addition, Scierka *et al.* proved by XPS that Cr is highly dispersed on an alumina surface and ISS results on the same catalysts show that the Cr phase covers only a small fraction of the alumina surface.<sup>108</sup> In conclusion, Cr<sup>6+</sup>, Cr<sup>5+</sup>, and Cr<sub>2</sub>O<sub>3</sub> clusters are formed on calcined surfaces, and their relative amounts and coordination geometries strongly depend on the support type and composition, the Cr loading, and heat treatment.

### 3. Reduced Cr

The reduction process of Cr and speciation of reduced Cr on amorphous supports have been extensively investigated by several spectroscopic and chemical techniques (mainly DRS, IR, ESR, EXAFS-XANES, XPS, and TPR). In general, three oxidation states, Cr<sup>2+</sup>, Cr<sup>3+</sup>, and Cr<sup>5+</sup>, are formed from Cr<sup>6+</sup>, with different coordination geometries and amounts.

DRS spectroscopy<sup>48,56–58</sup> show the presence of three new species: (pseudo-) octahedral Cr<sup>2+</sup>, (pseudo-) tetrahedral Cr<sup>2+</sup>, and (pseudo-) octahedral Cr<sup>3+</sup>, their relative concentration depending on the treatment and the support composition. The spectroscopic fingerprints of these reduced Cr species are summarized in Table 2. In principle, Cr<sup>5+</sup> could also be detected by DRS, but the amounts are too small for detection.

IR and EXAFS spectroscopies<sup>69–72,93</sup> show that a fraction of the Cr<sup>2+</sup> and Cr<sup>3+</sup> ions possess a low coordination number and because the latter technique only reveals a mean coordination environment, it is less informative. Instead, IR spectroscopy has shown to be a very powerful technique due to its

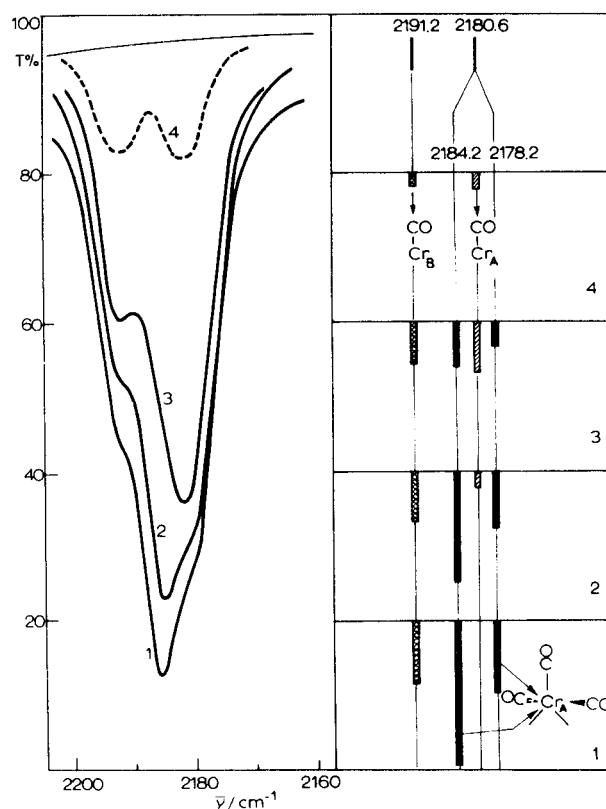


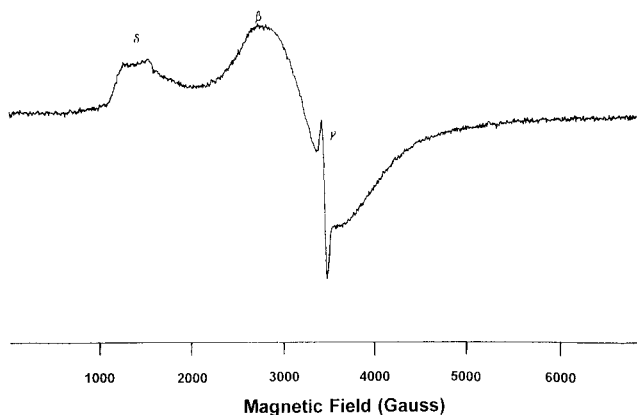
**Figure 9.** IR spectra of adsorbed CO on a reduced Cr/SiO<sub>2</sub> catalyst and schematic interpretation. Equilibrium pressures: curve 1, 40 torr; curve 2, 0.4 torr; curve 3, 0.2 torr; curve 4, 6 min pumping. (Reprinted from ref 75. Copyright 1988 Elsevier Science Publishers.)

ability to discriminate between different surface Cr<sup>2+</sup> species.<sup>69–85</sup> This is illustrated in Figure 9 for CO reduced Cr/SiO<sub>2</sub> catalysts.<sup>77</sup> Three families of anchored Cr<sup>2+</sup> ions have been singled out (labeled as A, B, and C), after chemisorption of CO. These three species differ in their degree of coordinative unsaturation (A < B < C) and consequently in their propensity to react (A > B > C). The corresponding CO IR bands are given in Table 2. It is also important to stress that IR is indirect since it cannot probe Cr sites directly.

Three different Cr species can be detected with ESR:<sup>34–47</sup> isolated Cr<sup>5+</sup> species, clustered Cr<sup>3+</sup>, and dispersed Cr<sup>3+</sup>. These three species are usually denoted as  $\gamma$ -signal,  $\beta$ -signal, and  $\delta$ -signal, respectively, and the spectroscopic characteristics are summarized in Table 2. A typical example of an X-band ESR spectrum is shown in Figure 10 for a supported Cr/Al<sub>2</sub>O<sub>3</sub> catalysts.<sup>46</sup> The  $\gamma$ -signal can be present under different coordinations, depending on the support composition. This is illustrated in Table 4. Two main Cr<sup>5+</sup> coordinations, with slightly different ESR parameters, are observed: i.e. square-pyramidal and pseudotetrahedral coordination. The  $\beta$ -signal is an isotropic signal, which is mainly present on reduced alumina surfaces, and its  $g$  value and line width strongly depend on the reduction temperature and Cr loading.<sup>46</sup> The  $\delta$ -signal is a special one because it has only a strong and broad positive lobe around  $g = 3.5–5.5$ . This signal, which follow the Curie–Weiss law, can be simulated by using high zero field parameters  $D$  and  $E$ , which mean that is due to an isolated strongly distorted Cr<sup>3+</sup> octahedron.<sup>46,47,106</sup>

**Table 4. Literature Survey of ESR Parameters of Cr<sup>5+</sup> and <sup>53</sup>Cr<sup>5+</sup> on Different Amorphous Supports and Their Assignments**

support	ESR parameters	assignments	ref(s)
SiO <sub>2</sub>	$g_{\parallel} = 1.975; g_{\perp} = 1.898$	pseudotetrahedral Cr <sup>5+</sup>	43
	$g_{\parallel} = 1.981; g_{\perp} = 1.901$	square-pyramidal Cr <sup>5+</sup>	46,47,106
	$g_{\parallel} = 1.939; g_{\perp} = 1.979$	square-pyramidal Cr <sup>5+</sup>	
	$g_{xx} = 1.978; g_{yy} = 1.969; g_{zz} = 1.895$	pseudotetrahedral Cr <sup>5+</sup>	
	$g_1 = 1.950; g_2 = 1.975; g_3 = 1.975; A_1 = 45 \text{ G}; A_2 = 14 \text{ G}; A_3 = 14 \text{ G}$	pseudotetrahedral <sup>53</sup> Cr <sup>5+</sup>	36
	$g_1 = 1.895; g_2 = 1.968; g_3 = 1.975; A_1 = 39 \text{ G}; A_2 = 18 \text{ G}; A_3 = 16 \text{ G}$	square-pyramidal <sup>53</sup> Cr <sup>5+</sup>	42
Al <sub>2</sub> O <sub>3</sub>	$g_{\perp} = 1.983; g_{\parallel} = 1.920$	square-pyramidal Cr <sup>5+</sup>	
	$g_{\parallel} = 1.978; g_{\perp} = 1.910$	square-pyramidal Cr <sup>5+</sup>	
	$g_{av} = 1.971$	square-pyramidal <sup>53</sup> Cr <sup>5+</sup>	36
SiO <sub>2</sub> ·Al <sub>2</sub> O <sub>3</sub>	$g_{\parallel} = 1.975; g_{\perp} = 1.910$	square-pyramidal Cr <sup>5+</sup>	46,47,106
TiO <sub>2</sub>	$g_{\parallel} = 1.975; g_{\perp} = 1.950$	square-pyramidal Cr <sup>5+</sup>	45
	$g_{\parallel} = 1.945; g_{\perp} = 1.977; A_{\parallel} = 46 \text{ G}; A_{\perp} = 14 \text{ G}$	square-pyramidal Cr <sup>5+</sup>	36
ZrO <sub>2</sub>	$g_{\parallel} = 1.953; g_{\perp} = 1.977; A_{\parallel} = 46 \text{ G}; A_{\perp} = 13 \text{ G}$	square-pyramidal Cr <sup>5+</sup>	36,37
SnO <sub>2</sub>	$g_{\parallel} = 1.955; g_{\perp} = 1.986; A_{\parallel} = 44 \text{ G}; A_{\perp} = 14 \text{ G}$	square-pyramidal Cr <sup>5+</sup>	36

**Figure 10.** X-band ESR spectrum of a supported Cr/Al<sub>2</sub>O<sub>3</sub> catalysts. (Reprinted from ref 64. Copyright 1995 American Chemical Society.)

XPS is a valuable tool for the discrimination between different reduced supported Cr ions and a number of interesting papers appeared in the literature.<sup>86–91</sup> The different binding energies corresponding to a particular Cr oxidation state are summarized in Table 2 although these values must be handled with care as explained in section III. Finally, chemical techniques, like TPR measurements, can be used to unravel the overall chemistry of the reduction process of supported Cr catalysts.<sup>109,110</sup> Recent TPR measurements on a series of supported Cr/SiO<sub>2</sub>·Al<sub>2</sub>O<sub>3</sub> catalysts with different SiO<sub>2</sub> content show that the mean oxidation state of Cr after reduction increases with increasing alumina content and Cr loading.<sup>93</sup> Thus, mainly Cr<sup>2+</sup> and Cr<sup>3+</sup> are formed on silica and alumina surfaces, respectively, while silica aluminas possess an intermediate Cr<sup>2+</sup>:Cr<sup>3+</sup> ratio on their surface.

In summary, by reduction Cr<sup>6+</sup> is converted to Cr<sup>5+</sup>, Cr<sup>3+</sup>, and Cr<sup>2+</sup>, each in different coordination environments and amounts. On silica, the Cr<sup>2+</sup> species is the main species, and three main families, differing in their degree of coordinative unsaturation, have been detected.

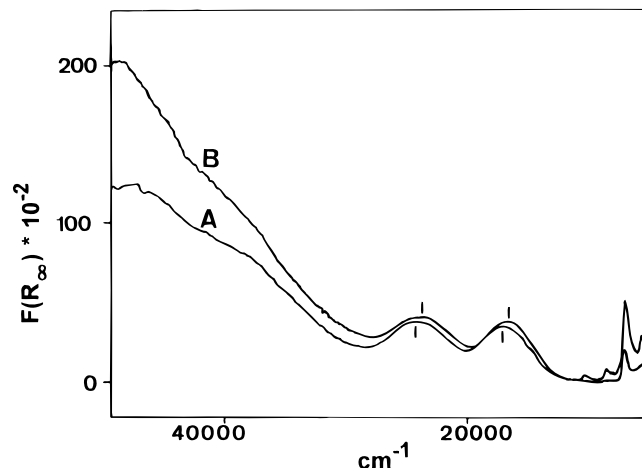
## B. Molecular Structure of Cr on Molecular Sieves

Chromium-containing molecular sieves can be prepared in three different ways: (1) by ion exchange with an aqueous chromium solution or by solid-state ion exchange using an appropriate chromium salt; (2) by impregnation with a chromium solution; and (3) by hydrothermal synthesis of a molecular sieve

in the presence of different chromium salts.<sup>106</sup> The surface chemistry of Cr<sup>n+</sup> (with  $n = 2, 3, 5,$  and  $6$ ) in molecular sieves is somewhat similar, regardless of the Cr loading, the type of immobilization, the molecular sieve structure type, and composition. This can be deduced from Tables 5 and 6, where the reported DRS and ESR results are presented, respectively. The studied molecular sieves are zeolite A, X, and Y; mordenite; ZSM-5; silicalite, and AIPO's. Two review papers have appeared in the literature about Cr molecular sieves: Kucherov and Slinkin recently reviewed their work about Cr in high-silica zeolites,<sup>132</sup> while a more general review was made in the early 1970s by Kazanskii and co-workers.<sup>118</sup>

### 1. Chromium Ion-Exchanged and -Impregnated Molecular Sieves

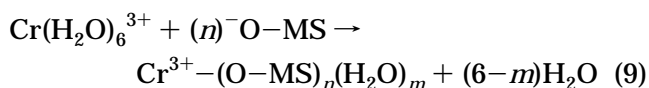
After ion exchange and impregnation, Cr<sup>3+</sup> or Cr<sup>2+</sup> ions are present as hexaquo complexes in the cages and channels of molecular sieves. This is illustrated by the DRS spectrum of a freshly prepared Cr<sup>3+</sup> zeolite in Figure 11, and the corresponding absorption bands are given in Table 5. Drying of these materials results in a decrease of the ligand field strength of the Cr(H<sub>2</sub>O)<sub>6</sub><sup>3+</sup> complex, as evidenced by the red shift of the d–d bands (Figure 11). This lowering is due to two phenomena: (a) the removal of water from the second coordination sphere of chromium and (b) the replacement of one (or more)

**Figure 11.** DRS spectra of hydrated and dried Cr-exchanged zeolite Y (with Ga substituted for Al): (A) freshly prepared and (B) after drying. (Reprinted from ref 120. Copyright 1994 Butterworths.)

**Table 5. Literature Survey of DRS Absorption Bands of Cr Containing Molecular Sieve and Their Assignments**

Cr containing molecular sieve (Cr loading/preparation method)	pretreatment	absorption bands (cm <sup>-1</sup> )	assignments	ref
Cr <sup>2+</sup> /NaA (1–3 Cr/UC; ion exchange)	hydrated	12000; 17000	Cr <sup>2+</sup> <sub>trig</sub>	111
Cr <sup>3+</sup> /NaL (1.33 Cr/UC; ion exchange)	hydrated	17400; 25000; 35800	Cr(H <sub>2</sub> O) <sub>6</sub> <sup>3+</sup>	112
	dehydrated	15000	Cr <sup>3+</sup> <sub>oct</sub>	
	calcined	26800; 36500	CrO <sub>4</sub> <sup>2-</sup>	
Cr <sup>3+</sup> /Na-mordenite (1.56 Cr/UC; ion exchange)	hydrated	17200; 24600; 35800	Cr(H <sub>2</sub> O) <sub>6</sub> <sup>3+</sup>	112
	dehydrated	15000	Cr <sup>3+</sup> <sub>oct</sub>	
	calcined	26800; 36500	CrO <sub>4</sub> <sup>2-</sup>	
Cr <sup>3+</sup> /NaY (3.9 Cr/UC; ion exchange)	hydrated	17200; 23800	Cr(H <sub>2</sub> O) <sub>6</sub> <sup>3+</sup>	113
	calcined	13900; 28600	Cr <sup>6+</sup>	
Cr <sup>3+</sup> /NaX (4.3 Cr/UC; ion exchange)	hydrated	17200; 23800	Cr(H <sub>2</sub> O) <sub>6</sub> <sup>3+</sup>	113
	calcined 300 °C	13900; 28600	Cr <sup>6+</sup>	
Cr <sup>3+</sup> /NaY (ion exchange)	hydrated	17200; 24400	Cr(H <sub>2</sub> O) <sub>6</sub> <sup>3+</sup>	114
	dehydrated 350 °C	13300	Cr <sup>2+</sup>	
Cr <sup>3+</sup> /NaY (0.39 Cr/UC; ion exchange)	dehydrated 20 °C	16100; 23800	Cr(H <sub>2</sub> O) <sub>6</sub> <sup>3+</sup>	115
	dehydrated 100 °C	15900; 23100	Cr <sup>3+</sup> <sub>oct</sub>	
	dehydrated 200 °C	8000; 9100; 15600; 20800	Cr <sup>2+</sup> <sub>tetr</sub> , Cr <sup>3+</sup> <sub>oct</sub>	
Cr <sup>2+</sup> /NaY (1.5 Cr/UC; ion exchange)	hydrated	14000	Cr(H <sub>2</sub> O) <sub>6</sub> <sup>2+</sup>	116
	dehydrated 350 °C	12300; 17000	Cr <sup>2+</sup> <sub>trig</sub>	
Cr <sup>3+</sup> /NaA, NaX and NaY (ion exchange)	hydrated	16000; 23550; 35100	Cr(H <sub>2</sub> O) <sub>6</sub> <sup>3+</sup>	117
Cr <sup>2+</sup> /NaY (ion exchange)	hydrated	13500	Cr(H <sub>2</sub> O) <sub>6</sub> <sup>2+</sup>	118
	dehydrated 300 °C	12600; 15200; 31000	Cr <sup>2+</sup> <sub>disoct</sub>	
Cr <sup>3+</sup> /NaY (4, 8, 15.8 Cr/UC; ion exchange)	hydrated	17100; 23800	Cr(H <sub>2</sub> O) <sub>6</sub> <sup>3+</sup>	119
	calcined 550 °C	17100; 22000; 27800; 37700	Cr <sup>3+</sup> <sub>oct</sub> , CrO <sub>4</sub> <sup>2-</sup>	
	dehydrated 450 °C	14200; 16400; 22400	Cr <sup>3+</sup> <sub>oct</sub>	
Cr <sup>3+</sup> /NaY (0.089–0.38 Cr/UC; ion exchange)	hydrated	17000; 24000; 33000	Cr(H <sub>2</sub> O) <sub>6</sub> <sup>3+</sup>	120
	calcined 550 °C	28000; 38000; 22500	chromate/dichromate	
	reduced	16000; 12600; 7600	Cr <sup>3+</sup> /Cr <sup>2+</sup>	
Cr <sup>3+</sup> /NaGaY (0.32–1.11 Cr/UC; ion exchange)	hydrated	17000; 24000; 33000	Cr(H <sub>2</sub> O) <sub>6</sub> <sup>3+</sup>	120
	calcined 550 °C	28000; 38000	chromate	
	reduced	16000; 12600; 7600	Cr <sup>3+</sup> /Cr <sup>2+</sup>	
Cr <sup>3+</sup> /NaX (0.093–0.34 Cr/UC; ion exchange)	hydrated	17000; 24000; 33000	Cr(H <sub>2</sub> O) <sub>6</sub> <sup>3+</sup>	120
	calcined 550 °C	28000; 38000	chromate	
	reduced	16000; 12600; 7600	Cr <sup>3+</sup> /Cr <sup>2+</sup>	
Cr <sup>3+</sup> /NaY (0.087–0.37 Cr/UC impregnation)	hydrated	17000; 24000; 33000	Cr(H <sub>2</sub> O) <sub>6</sub> <sup>3+</sup>	120
	calcined 550 °C	28000; 38000; 22500	chromate/dichromate	
	reduced	16000; 12600; 7600	Cr <sup>3+</sup> /Cr <sup>2+</sup>	
Cr <sup>3+</sup> /HY (0.09–0.56 wt %; solid state ion exchange)	hydrated	17000; 24000; 33000	Cr(H <sub>2</sub> O) <sub>6</sub> <sup>3+</sup>	120
	calcined 550 °C	28000; 38000; 10000	chromate	
	reduced	15000; 19500; 10000	Cr <sup>3+</sup> /Cr <sup>2+</sup>	
Cr-SAPO-34 (hydrothermally synthesised)	as-synthesized	15000; 17400; 23800	Cr <sup>3+</sup> <sub>oct</sub>	121
Cr silicalite (hydrothermally synthesised)	as-synthesized	22700; 15600	Cr <sup>3+</sup> <sub>oct</sub>	122,123
	calcined	27000	Cr <sup>6+</sup>	
CrAPO-5 (hydrothermally synthesized)	calcined	37000; 29400	Cr <sup>6+</sup>	124
CrAPO-5 (hydrothermally synthesized)	as-synthesized	15900; 21800; 33000	Cr <sup>3+</sup> <sub>oct</sub>	125
	calcined	29100; 36100	chromate	
	reduced	19400; 14200; 12500; 8400	Cr <sup>2+</sup> /Cr <sup>3+</sup>	
Cr silicalite (hydrothermally synthesized)	as-synthesized	16000; 22700; 33000	Cr <sup>3+</sup> <sub>oct</sub>	126
	calcined	28300; 40000	chromate/dichromate	
	reduced	12000; 7500	Cr <sup>2+</sup>	
Cr <sup>3+</sup> /Mordenite (0.14–0.31 Cr/UC; ion exchange)	hydrated	17000; 24000; 33000	Cr(H <sub>2</sub> O) <sub>6</sub> <sup>3+</sup>	120
	calcined 550 °C	28000; 38000	chromate	
	reduced	15000	Cr <sup>3+</sup> /Cr <sup>2+</sup>	

water molecule(s) in the first coordination sphere of the Cr<sup>3+</sup> ion by a weaker ligand, e.g. the lattice oxygen of the molecular sieve.<sup>125</sup> This process can be visualized, for Cr<sup>3+</sup>-exchanged molecular sieves (MS), in the following way:



The location and nature of the Cr<sup>3+</sup> complexes after impregnation of the molecular sieve or after mixing of the molecular sieve with a chromium salt (for solid-state ion exchange) is not known, but appreciable quantities of Cr may be on the external surface of the molecular sieve.<sup>106</sup>

Upon calcination, these hydrated Cr<sup>3+</sup> and Cr<sup>2+</sup> complexes are oxidized to chromate, dichromate, or

polychromate (Cr<sup>6+</sup>), chromyl cations (Cr<sup>5+</sup>), and some Cr<sub>2</sub>O<sub>3</sub> clusters (Cr<sup>3+</sup>).<sup>106</sup> Chromate is an anionic species and the stabilization in the anionic molecular sieve structure can only be explained by an anchoring reaction with two oxygens of the molecular sieve.<sup>126</sup> This reaction also results in the formation of two extra framework oxygens,<sup>123</sup> and such a mechanism is very similar to that proposed for amorphous supports. Recently, the group of Zecchina has shown that nests of hydroxyl groups inside silicalite molecular sieves can react with chromic acid to give anchored (grafted) monochromate and/or dichromate and this reaction must also occur upon calcination of Cr-exchanged or -impregnated molecular sieves.<sup>133,134</sup> Finally, considerable amounts of dichromate and polychromates are observed on impregnated Cr molecular sieves, where Cr<sup>6+</sup> ions are

**Table 6. Literature Survey of ESR Signals of Cr<sup>3+</sup> and Cr<sup>5+</sup> in Chromium Containing Molecular Sieve and Their Assignments**

chromium-containing molecular sieve	treatment	ESR signal	assignment	ref(s)
ion-exchanged Cr-Y	hydrated calcined	$g_{\text{eff}} = 1.965$ $g_{\perp} = 1.987$ ; $g_{\parallel} = 1.940$  $g_{\perp} = 1.980$ ; $g_{\parallel} = 1.915$	Cr(H <sub>2</sub> O) <sub>x</sub> (Z-O <sup>-</sup> ) with Z = zeolite Y Y <sub>1</sub> signal: [Cr=O] <sup>3+</sup> ion at site II (supercage) Y <sub>2</sub> signal: [Cr=O] <sup>3+</sup> ion at site I' or II' (small cages)	127,128
ion-exchanged Cr mordenite	calcined	$g_{xx} = 1.9867$ ; $g_{yy} = 1.9720$ ; $g_{zz} = 1.9110$ $g_{\perp} = 1.9947$ ; $g_{\parallel} = 1.9070$	A signal: square-pyramidal [Cr=O] <sup>3+</sup> ion in the main channel B signal: distorted tetrahedral [Cr=O] <sup>3+</sup> ion at junction between main channel and the sidepocket	129
ion-exchanged Cr-X	calcined	$g_{\perp} = 1.99$ ; $g_{\parallel} = 1.93$	[Cr=O] <sup>3+</sup> ion	106,126
ion-exchanged Cr-GaY	calcined	$g_{\perp} = 1.99$ ; $g_{\parallel} = 1.94$	Y <sub>1</sub> signal	106,126
solid-state-ion exchanged Cr-Y	calcined	$g_{\perp} = 1.98$ ; $g_{\parallel} = 1.94$	Y <sub>2</sub> signal	106,126
		$g_{\perp} = 1.99$ ; $g_{\parallel} = 1.93$	Y <sub>1</sub> signal	
impregnated Cr-Y	calcined	$g_{\perp} = 1.98$ ; $g_{\parallel} = 1.94$	Y <sub>1</sub> signal	106,126
		$g_{\perp} = 1.98$ ; $g_{\parallel} = 1.92$	Y <sub>2</sub> signal	
ion-exchanged Cr-Y	calcined	$g_{\perp} = 1.99$ ; $g_{\parallel} = 1.95$	Y <sub>1</sub> signal	106,126
		$g_{\perp} = 1.98$ ; $g_{\parallel} = 1.92$	Y <sub>2</sub> signal	
ion-exchanged Cr-Y	hydrated calcined	$g_{\perp} = 1.99$ ; $g_{\parallel} = 1.95$	Y <sub>1</sub> signal	106,126
		$g_{\text{av}} = 2.0$	Cr(H <sub>2</sub> O) <sub>6</sub> <sup>3+</sup>	
CrAPO-5	hydrated	$g_{\perp} = 1.991$ ; $g_{\parallel} = 1.910$ $g_{\perp} = 1.991$ ; $g_{\parallel} = 1.883$	Y <sub>1</sub> signal Y <sub>2</sub> signal	113
		$g_{\text{av}} = 1.987$ $g_{xx} = 1.987$ ; $g_{yy} = g_{zz} = 1.865$ ; $D = 0.490 \text{ cm}^{-1}$ ; $E = 0.163 \text{ cm}^{-1}$	signal A: Cr(H <sub>2</sub> O) <sub>6</sub> <sup>3+</sup> signal B: Cr <sup>3+</sup> dispersed	
Cr silicalite	as-synthesized	$g_{\perp} = 1.99$ ; $g_{\parallel} = 1.90$ $g_{\text{av}} = 2.0$	signal C: Cr <sup>5+</sup> signal D: Cr <sub>2</sub> O <sub>3</sub>	130
		$g_{xx} = 4.49$ ; $g_{yy} = 2.71$ ; $g_{zz} = 1.66$ $g_{xx} = 2.00$ ; $g_{yy} = 1.67$ ; $g_{zz} = 1.66$ $g_{\text{av}} = 2.08$	signal A: substitutional site signal B: substitutional site signal C: Cr(H <sub>2</sub> O) <sub>3</sub> <sup>6+</sup>	
Cr silicalite	hydrated	$g_{\text{av}} = 2.0$	Cr(H <sub>2</sub> O) <sub>6</sub> <sup>3+</sup>	126
Cr silicalite	calcined	$g_{\text{av}} = 2.0$	Cr <sup>5+</sup>	131
	hydrated calcined	$g_{\text{av}} = 1.976$ $g_{\text{av}} = 1.979$	Cr(H <sub>2</sub> O) <sub>6</sub> <sup>3+</sup> or Cr <sub>2</sub> O <sub>3</sub> Cr <sup>5+</sup>	

partially located at the external surface of the molecular sieve crystals.<sup>106</sup>

The surface chemistry of Cr<sup>5+</sup> in molecular sieves is more diverse and chromyl cations can be present under different coordination geometries and at different cationic sites, as illustrated in Table 6. The two same coordination environments as for amorphous supports are proposed: square pyramidal and pseudotetrahedral. The Cr<sup>5+</sup> species in mordenite-type molecular sieves are an interesting example since it is characterized by a complex ESR spectrum (Figure 12) possessing two rhombic signals with one exhibiting aluminum superhyperfine splitting (species B). The simulated spectrum, together with the individual components A and B, is also shown in Figure 12, and is very close to the experimental one.<sup>106,47</sup> Species A is assigned to Cr<sup>5+</sup> ions present at the junction between the main channel and the side pocket, while species B is located near a framework aluminum in the main channel of mordenite molecular sieves.<sup>129</sup>

These Cr<sup>6+</sup> and Cr<sup>5+</sup> complexes are reducible to pseudooctahedral Cr<sup>3+</sup> and pseudotetrahedral and pseudooctahedral Cr<sup>2+</sup>, depending on the preparation method, treatment, and the molecular sieve type and composition. The DRS absorption bands of reduced Cr on amorphous supports are included in Table 5 and are somewhat similar to those observed for reduced Cr on amorphous supports. For a state of the art of the chemistry and spectroscopy of solid-state ion-exchanged Cr molecular sieves, we refer to a recent review of Kucherov and Slinkin.<sup>132</sup>

Quantum-chemical calculations were used by the group of Wichterlova for the calculation of the physicochemical properties of Cr<sup>2+</sup>, Cr<sup>3+</sup>, Cr<sup>5+</sup>, and Cr<sup>6+</sup>

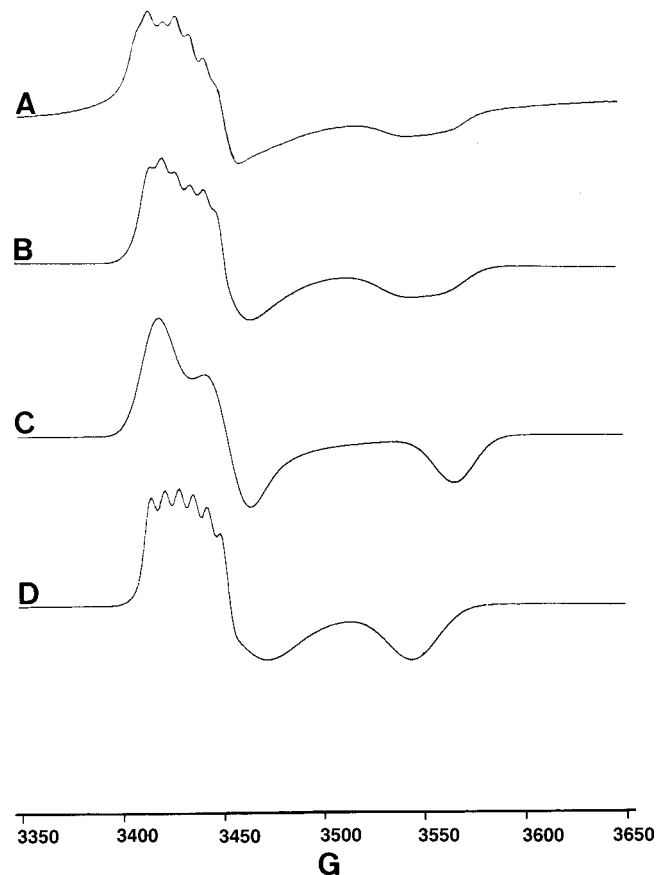


**Figure 12.** ESR spectra of calcined Cr mordenite: (A) experimental spectrum; (B) overall simulated spectrum (by an appropriate summation of the spectra of species A and B); (C) simulated spectrum of species A; and (D) simulated spectrum of species B. (Reprinted from ref 47. Copyright 1996 Royal Chemical Society.)

at site II (supercage) in faujasite zeolites, modeled by  $\text{Si}_3\text{Al}_3\text{O}_6(\text{OH})_{12}\text{Cr}$  clusters.<sup>135</sup> They show that the Cr ions are bonded to the molecular sieve skeleton by electron donor-acceptor bonds whose formation lead to electron donation from the skeleton to the cation, thus stabilizing the valence states of the Cr ions. The most probable valence state of the Cr ions in the zeolites was found to be  $\text{Cr}^{3+}$ ; however, it can readily be oxidized to  $\text{Cr}^{5+}$  and  $\text{Cr}^{6+}$ . These ions were found to exhibit high electron-acceptor ability and thus are easily reduced away.

Detailed information about the coordination environment of  $\text{Cr}^{n+}$  in zeolites X, Y, and A has been obtained by using nitric oxide as a chemical probe and the obtained chromium-nitrosyl complexes were characterized by a combined IR-ESR spectroscopies. In the 1970s, Naccache and Taarit and Chambellan *et al.* showed that  $\text{Cr}^{3+}$  exchanged zeolites can be either oxidized to  $\text{Cr}^{5+}$  by oxygen or reduced by  $\text{H}_2$  or CO to mainly  $\text{Cr}^{2+}$ .<sup>121,122</sup> The latter species forms stable NO complexes of the type  $\text{Cr}^{\text{I}}-\text{NO}^+$ , i.e. mononitrosyl complexes of  $\text{Cr}^{2+}$ , giving rise to axial ESR signals with  $g_{\perp} = 1.977$  and  $g_{\parallel} = 1.846-1.917$ . Pearce *et al.* have reinvestigated these systems and concluded that their IR and ESR parameters are typical for a  $\text{Cr}^{\text{III}}(\text{NO})_2$  species, i.e. a dinitrosyl complex of  $\text{Cr}^{3+}$ .<sup>113</sup> Molecular orbital calculations on several model systems support this assignment.

In conclusion, the surface chemistry of Cr on zeolitic surfaces is quite similar to that observed for amorphous supports as the same coordination environments and oxidation states are revealed by spectroscopy.

## 2. Hydrothermally Synthesized, Chromium-Containing Molecular Sieves

The synthesis and characterization of chromium-substituted molecular sieves have only recently received special attention from researchers working in the field of molecular sieve science. Consequently, only a limited number of detailed papers<sup>123-126,130-131,137-141</sup> and some patents<sup>142-143</sup> have appeared in the literature, which report the synthesis and characterization of Cr-containing AlPO's (CrAPO-*n*) and silicalite (Cr silicalite) materials. The applied characterization techniques for studying these crystalline materials are XRD, SEM, DRS, ESR, NMR, and IR.

The key question here is if  $\text{Cr}^{3+}$  really substitutes in the framework of molecular sieves and to what extent. Isomorphous substitution requires tetrahedral  $\text{Cr}^{3+}$ , which is difficult to obtain because of the high crystal field stabilization energies of octahedral  $\text{Cr}^{3+}$  complexes. This is evidenced by the scarcity of tetrahedral  $\text{Cr}^{3+}$  complexes and the absence of reported inorganic structures with tetrahedral  $\text{Cr}^{3+}$ .<sup>106</sup>

In the acid synthesis gels of CrAPO-5 molecular sieves,<sup>125</sup> Cr is present as an octahedral Cr-aquo complex (for  $\text{Cr}^{3+}$ ) or chromate and polychromate (for  $\text{Cr}^{6+}$ ). In the case of Cr silicalite gels, which have a basic pH, the  $\text{Cr}^{3+}$  ions are present as polymerized octahedrally coordinated ions and as chromate anions for  $\text{Cr}^{6+}$ . Thus, the same chemistry is revealed in the synthesis gels as in aqueous solutions. Consequently, these ions are in the liquid phase of the gel and can be easily washed off.

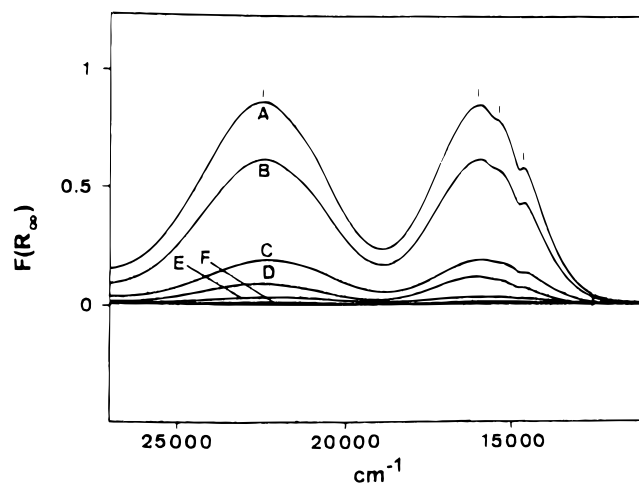


**Figure 13.** DRS spectra of as-synthesized CrAPO-5 molecular sieves with increasing Cr content: 0.75  $\text{Et}_3\text{N}$ . ( $\text{Cr}_x\text{Al}_x\text{P}_x\text{O}_4 \cdot 20\text{H}_2\text{O}$  with  $x = 0.080$  (A); 0.040 (B); 0.020 (C); 0.004 (D); 0.002 (E); and 0.000 (F) (Reprinted from ref 125. Copyright 1994 Butterworths).

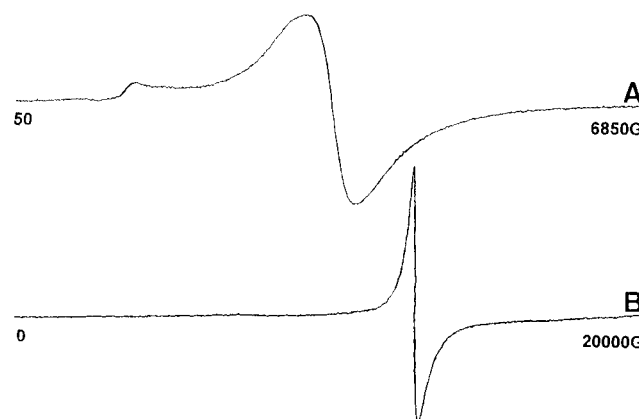


**Figure 14.** ESR spectra of as-synthesized CrAPO-5 molecular sieves measured at 300 K: (A) X-band spectrum and (B) Q-band spectrum. (Reprinted from ref 47. Copyright 1996 Royal Chemical Society.)

During and after hydrothermal synthesis, Cr is present as  $\text{Cr}^{3+}$  in (pseudo-) octahedral coordination to oxygen.<sup>125-126</sup> This is illustrated in Figures 13 and 14 by some DRS and ESR spectra of as-synthesized CrAPO-5 molecular sieves. DRS shows two absorption bands at 15 900 and 21 800  $\text{cm}^{-1}$ , while in X-band and Q-band ESR an intense and broad signal around  $g = 2$  is detected. Both observations are characteristic of the presence of  $\text{Cr}^{3+}$  ions, surrounded by six oxygen ligands in octahedral coordination. Besides this signal, a broad and positive lobe around  $g = 4$  is observed. This signal has some similarities with the  $\delta$ -signal on amorphous supports and can be simulated by using high zero field parameters  $D$  and  $E$ . In view of the work on Cr silicalite of Nakamura *et al.*,<sup>130</sup> lattice-substituted  $\text{Cr}^{3+}$  cannot be excluded. Also Mosser *et al.*<sup>144</sup> and Gaité and Mosser<sup>145</sup> have shown that pseudooctahedral  $\text{Cr}^{3+}$  in kaolinite materials gives a  $g = 4.0$  signal.

Upon calcination, this  $\text{Cr}^{3+}$  is oxidized to mainly monochromate/polychromate and some  $\text{Cr}^{5+}$ , while reduction results in the formation of (pseudo-) octahedral  $\text{Cr}^{3+}$ , (pseudo-) octahedral  $\text{Cr}^{2+}$  and (pseudo-) tetrahedral  $\text{Cr}^{2+}$ .<sup>125-126</sup> In the case of calcined Cr

silicalite, Cr can be easily washed off from the crystalline material, suggesting a weak interaction between silicalite and Cr and a high solubility of Cr in the aqueous phase.<sup>123</sup> Although several authors<sup>123–124,130–131</sup> claim the isomorphous substitution of Cr in molecular sieves, no spectroscopic signatures of lattice substituted Cr have been available up to now in the literature. Only for CrAPO-14, an aluminophosphate with octahedral framework sites, is it clearly shown by single crystal XRD measurements that 4–5% of the octahedral sites are occupied by Cr<sup>3+</sup> ions.<sup>137</sup>

## V. Quantitation of Cr Species on Oxidic Surfaces

From the previous section it can be concluded that a qualitative picture of the surface chemistry of Cr emerges by applying different complementary characterization techniques. However, if one ever wants to develop structure/composition–reactivity relationships, quantitative measurements are necessary. Therefore, we have recently developed a novel spectroscopic method for the quantitation of Cr<sup>*n*+</sup> species (with *n* = 2, 3, 5, and 6) in inorganic oxides.<sup>46,56–57,120,126</sup>

The general approach of this method and the different steps in the quantitation are shown in Figure 15. The method is based on a detailed analysis of DRS and ESR spectra, which were taken as a function of one parameter (reduction temperature, Cr loading, or support composition). In a second step, the obtained spectra were decomposed into their individual components, belonging to a particular oxidation state. Chemometric techniques (e.g. SIMPLISMA, simple to use interactive self-modeling mixture analysis) and ESR simulations are useful in this respect because they are able to verify the presence of each proposed pure spectrum. In a final step, the individual oxidation states are quantified.

The application of this method on the DRS and ESR spectra of Cr/Al<sub>2</sub>O<sub>3</sub> catalysts as a function of the reduction temperature is shown in Figure 16. DRS spectroscopy reveal three pure species: chromate, octahedral Cr<sup>3+</sup>, and octahedral Cr<sup>2+</sup>, whereas with ESR square-pyramidal Cr<sup>5+</sup> is detected. This is shown in Figure 16, parts II and III. The calibration lines for Cr<sup>6+</sup> and Cr<sup>3+</sup> on alumina are given in Figure 16IV. The calibration line for Cr<sup>6+</sup> is almost linear, while the Cr<sup>3+</sup> calibration line is curved. Quantitation, which is only accurate between 0 and 0.4 wt % Cr, gives the concentration of Cr<sup>6+</sup>, Cr<sup>5+</sup>, Cr<sup>3+</sup>, and Cr<sup>2+</sup> after different pretreatments. This is illustrated in Figure 16V. After calcination Cr<sup>6+</sup> is the dominant species and only traces of Cr<sup>5+</sup> are present. After reduction, Cr<sup>6+</sup> is converted to mainly Cr<sup>3+</sup> and some Cr<sup>5+</sup> and Cr<sup>2+</sup>. In any case, the highest detected amounts of Cr<sup>5+</sup> are only 2–3% of the total Cr content.<sup>46</sup> Upon recalcination, Cr<sup>*n*+</sup> is partially reoxidized to Cr<sup>6+</sup> and a considerable amount is stabilized under Cr<sub>2</sub>O<sub>3</sub> form or dissolved in the alumina support.<sup>56</sup>

The developed method is also applicable to Cr/SiO<sub>2</sub> and Cr/SiO<sub>2</sub>·Al<sub>2</sub>O<sub>3</sub> catalysts, at least for low Cr loadings (<0.2 wt % Cr), but the analysis is always less accurate due to the coexistence of many coordination and oxidation states of Cr. Comparison between the different amorphous supports indicates that the Cr<sup>2+</sup>:Cr<sup>3+</sup> ratio increases with increasing

silica content of the support. Thus, silica-rich surfaces prefer Cr<sup>2+</sup> ions, while on alumina mainly Cr<sup>3+</sup> is present.<sup>56–57</sup> The same general trend is observed for chromium-containing molecular sieves: Cr<sup>6+</sup> ions are more easily reduced to Cr<sup>3+/2+</sup> in silica-rich than in alumina-rich and gallium-rich molecular sieves.<sup>120</sup>

All these observations are in line with TPR investigations on the same set of samples.<sup>93</sup> Thus, an average oxidation number of 2 and 3 was obtained after reduction for silica and alumina surfaces, respectively. Silica aluminas have an intermediate behavior. These differences in redox behavior can be explained in terms of hardness and softness, first introduced by Pearson.<sup>146</sup> Chemically softer oxides (silicon-rich) facilitate reduction of Cr (more Cr<sup>2+</sup> after reduction), while chemically harder oxides (aluminum- and gallium-rich) retard reduction (more Cr<sup>3+</sup> after reduction). This explanation has been proven recently by electronegativity equalization method based calculations.<sup>147</sup>

It is also important to stress here that the amount of ESR visible Cr<sup>5+</sup> ions on oxidic surfaces never exceeds more than 3% of the total Cr content, independent of the oxidic composition and structure, the Cr loadings and the applied treatment.<sup>46,106,126</sup> The amount of Cr<sup>5+</sup> on oxidic surfaces can be maximized by applying low Cr loadings and relatively low reduction treatments, and by using alumina-rich silica alumina oxides.<sup>46</sup>

An example of the introduction of chemometric techniques<sup>106,148</sup> in spectral analysis is given in Figure 17 for DRS spectra of hydrated Cr/SiO<sub>2</sub>·Al<sub>2</sub>O<sub>3</sub> catalysts as a function of the SiO<sub>2</sub> content. Four pure spectra are revealed in the spectra of the supported Cr catalysts: component A with three characteristic bands at 20 300, 30 600, and 44 100 cm<sup>-1</sup>; component B with three bands at 24 900, 36 600, and 45 500 cm<sup>-1</sup>; component C appeared at 17 700 cm<sup>-1</sup>, and component D absorbs in the region 28 600–37 000–49 000 cm<sup>-1</sup>. Components A and B are due to chromate and dichromate, respectively, and their relative ratio increases with decreasing silica content of the support. Component C is assigned to pseudooctahedrally coordinated Cr<sup>3+</sup>, while component D is a support band. The same analysis can be successfully applied on calcined and reduced supported Cr catalysts,<sup>106,148</sup> and the same kind of information is obtained as with spectral decomposition routines.

Thus, a set of spectroscopic and mathematical tools have become available in the literature, which allows one to tackle not only the speciation of Cr, but also to quantify the different oxidation states of Cr at least for low Cr loadings. Higher Cr loadings are better studied by X-ray photoelectron spectroscopy and a quantitative method has been developed by the group of Hercules and Houalla. This approach, based on the extensive use of chemometrical techniques, has been reviewed recently by Hercules *et al.*<sup>90</sup>

## VI. Mobility and Surface Reactivity of Cr on Oxidic Surfaces

### A. Mobility of Supported Cr

Chromium ions are often considered as contaminants in waste waters and in waste products of industries because of its use in various industrial

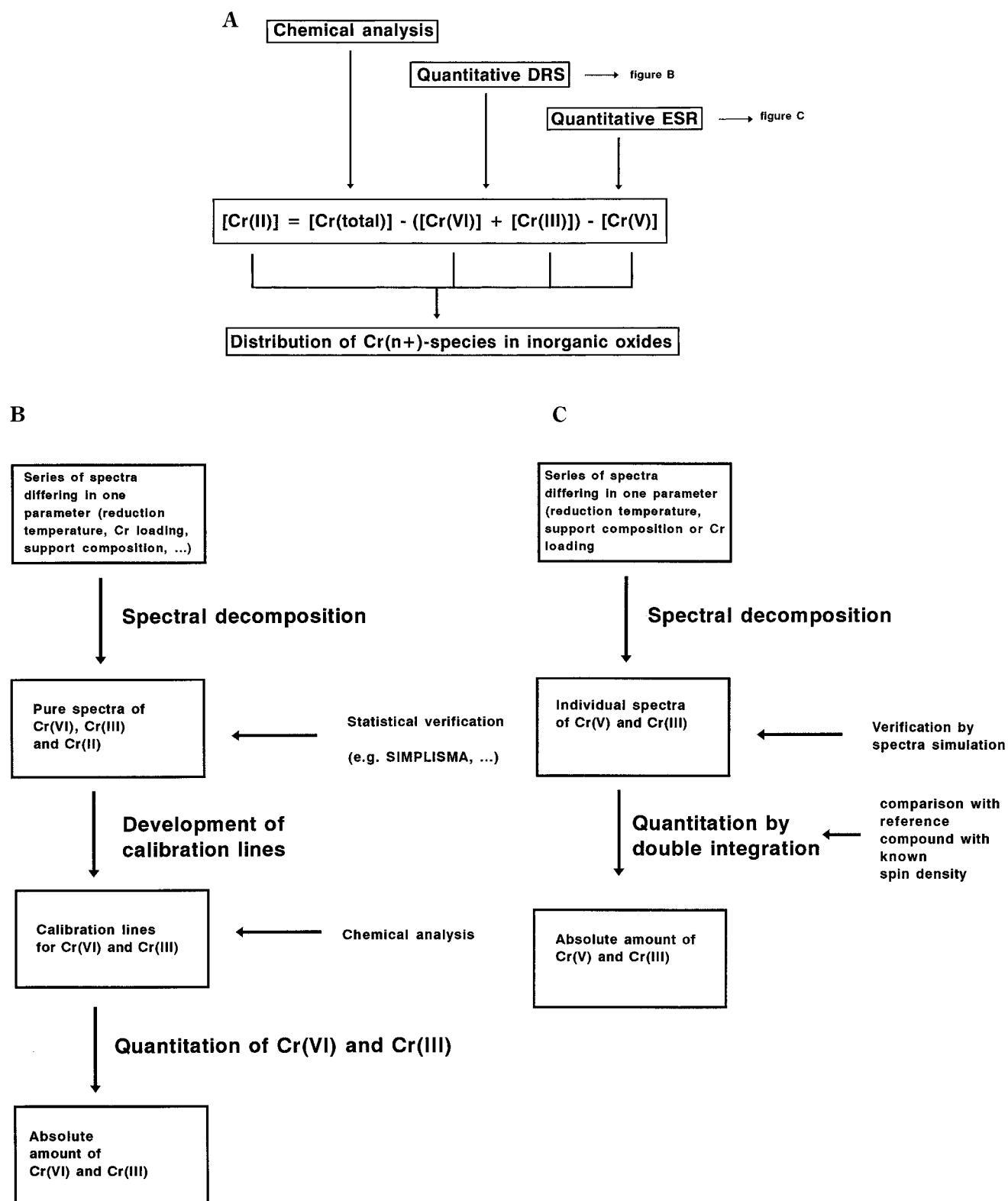


**Figure 15.** Combined DRS-ESR method for the quantitation of different Cr oxidation states: (A) overview of the combined quantitative DRS-ESR method; (B) quantitative DRS, and (C) quantitative ESR.

processes: e.g. Cr<sup>3+</sup> ions in waste waters and solid wastes of leather tanning manufacturers and Cr<sup>6+</sup> ions in waters of cooling towers.<sup>8,9</sup> The released ions are then immobilized in or on sediments/soils or taken up by microorganisms, plants, and animals.<sup>5</sup> The latter phenomenon is especially important because of the toxicity of Cr. To solve these problems, Cr wastes are often concentrated from waste waters or directly used for incorporation in cements. The obtained waste containers are then stored in disposal

sites. However, the immobilized chromium can be leached out by degradation of the cement matrices. Recent results on cementing of Cr show that (1) Cr<sup>3+</sup> ions are better retained in cement matrices than Cr<sup>6+</sup>, the leaching of which is a serious problem and (2) Cr retention is improved by addition of aluminum. Cr<sup>3+</sup> ions, released in the environment, are adsorbed on soil constituents, while the highly mobile Cr<sup>6+</sup> ions can be leached out and contaminate ground and surface waters.<sup>2,5</sup> On the other hand, the presence

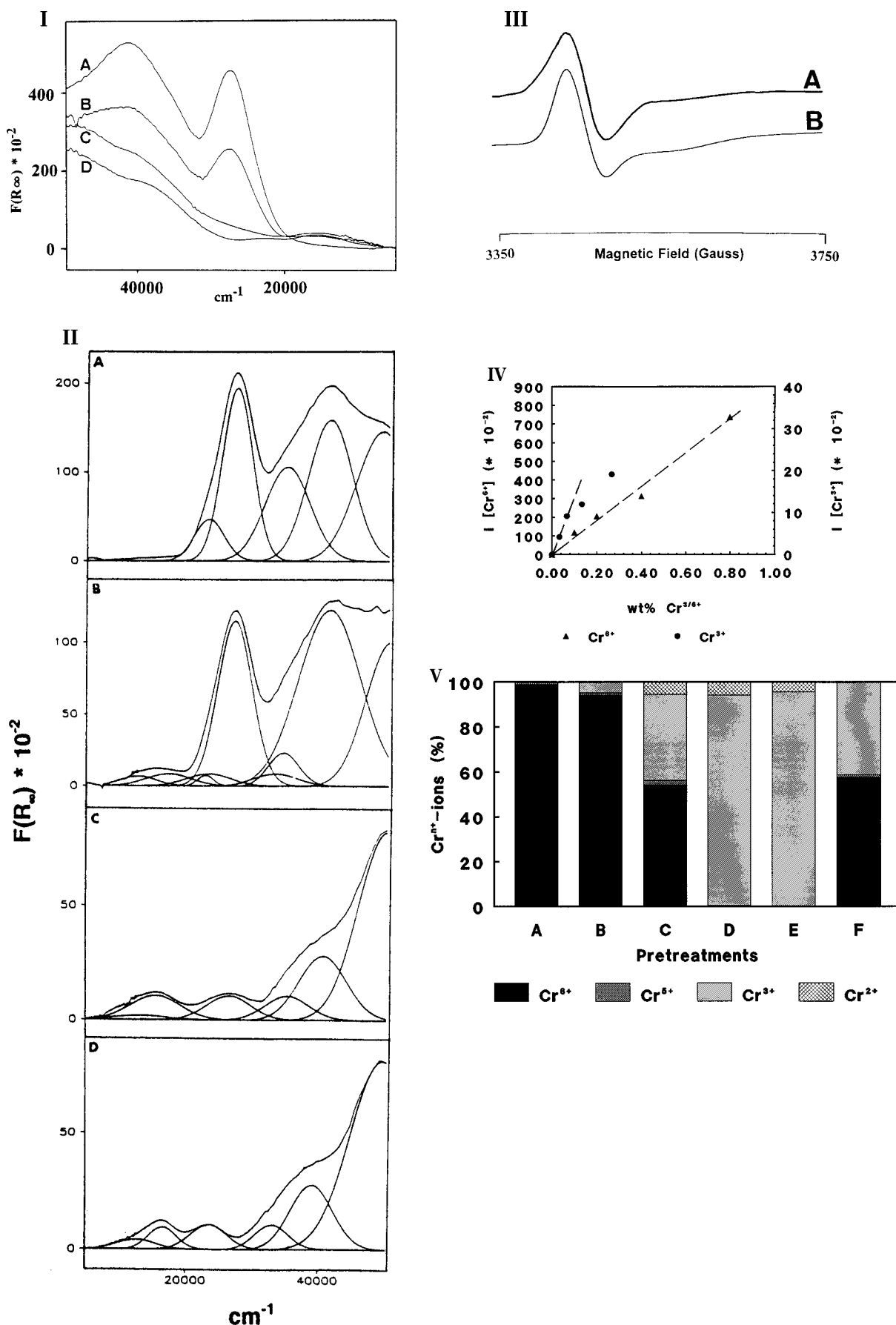


**Figure 16.** Application of the combined DRS-ESR method on the spectra of  $\text{Cr}/\text{Al}_2\text{O}_3$  catalysts as a function of reduction temperature: (I) Series of DRS spectra with increasing reduction temperature [reduction at 200 C (A); 300 C (B); 400 C (C) and 600 C (D)]; (II) deconvoluted diffuse reflectance spectra (same abbreviations as under I); (III) experimental (A) and simulated (B) ESR spectrum of  $\text{Cr}^{5+}$  on alumina; (IV) DRS calibration lines of  $\text{Cr}^{6+}$  and  $\text{Cr}^{3+}$ ; (V) distribution of  $\text{Cr}^{6+}$ ,  $\text{Cr}^{5+}$ ,  $\text{Cr}^{3+}$ , and  $\text{Cr}^{2+}$  ions on alumina as a function of pretreatment [(A) calcination at 550 °C; (B) reduction at 200 °C; (C) reduction at 300 °C, (D) reduction at 400 °C; (E) reduction at 600 °C; and (F) recalcination at 550 °C]. (Reprinted from refs 46 and 56. Copyright 1995 and 1993 American Chemical Society, respectively.)

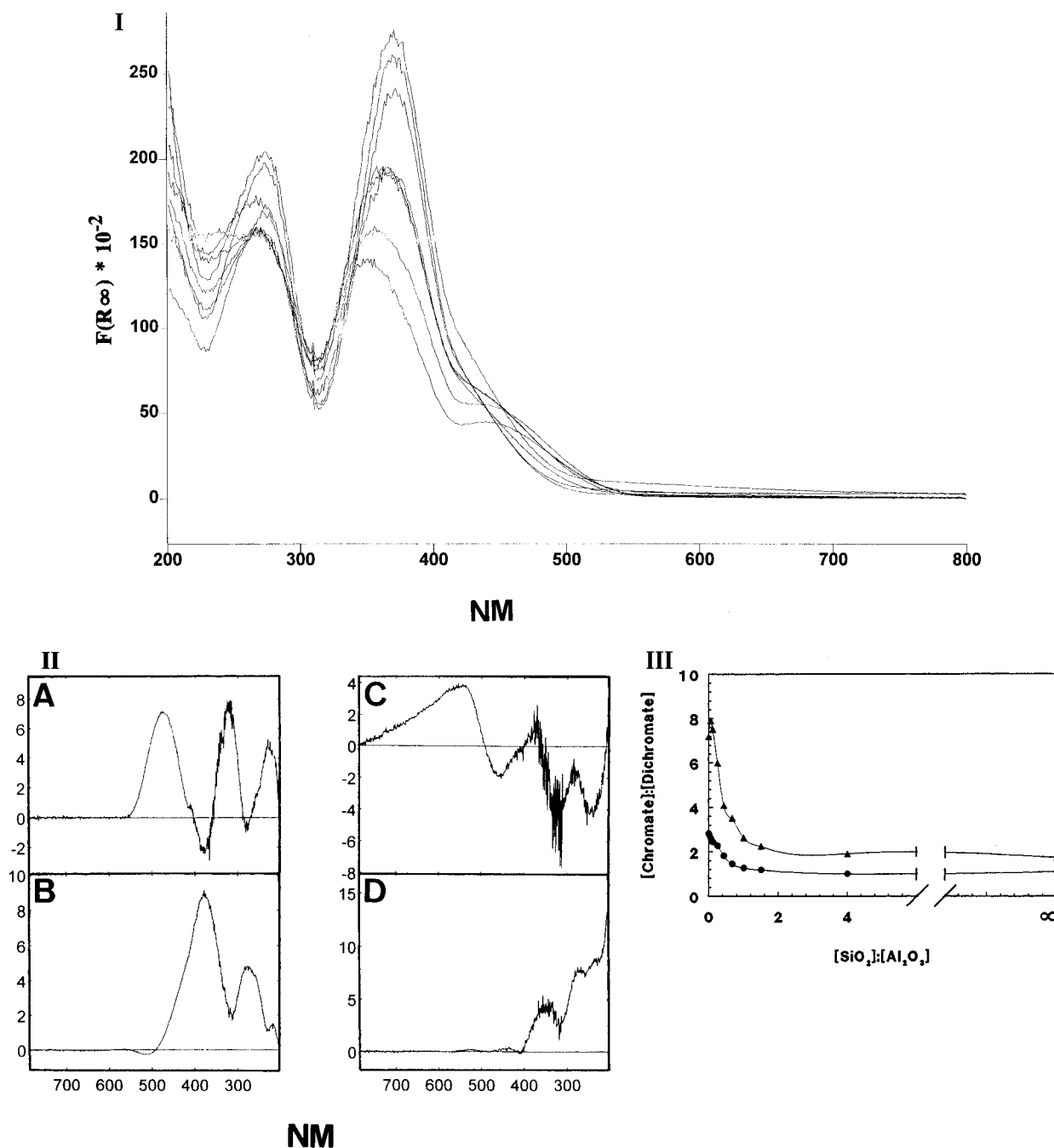


**Figure 17.** SIMPLISMA approach applied on DRS spectra of hydrated  $\text{Cr}/\text{SiO}_2 \cdot \text{Al}_2\text{O}_3$  catalysts: (I) series of DRS spectra of supported Cr catalysts with different  $\text{SiO}_2$  content; (II) pure spectra of dichromate (A), chromate (B),  $\text{Cr}^{3+}$  (C), and support (D); (III) chromate:dichromate ratio on silica aluminas as a function of the Si:Al ratio for hydrated ( $\blacktriangle$ ) and dehydrated ( $\bullet$ ) catalysts. (Redrawn from ref 106.)

of Cr in the feed of chemical reactors may deteriorate and/or inactivate heterogeneous catalysts, like fluid catalytic cracking catalysts, by migration of Cr toward catalytically active sites at high temperature or structural breakdown.<sup>149</sup>

All these studies show that Cr ions are mobile on hydrated and dehydrated surfaces with some preference for some inorganic oxides above others. This was recently confirmed by chemical analysis and by spectroscopy on Cr loaded silica, alumina, zeolite Y, and mordenite.<sup>67,150</sup> In dilute solution, silica and alumina have only a small affinity for Cr, be it either  $\text{Cr}^{3+}$  and  $\text{Cr}^{6+}$ . Molecular sieves show, however, a high preference for  $\text{Cr}^{3+}$  due to ion exchange, but the amount of  $\text{Cr}^{6+}$  taken up by these materials is always low. This is, of course, due to the cation exchange properties of molecular sieves.

Interesting results were obtained by mixing  $\text{Cr}^{3+/6+}$  oxide materials with an equal amount of an unloaded support. After calcination, the position of Cr was evaluated by DRS ( $\text{Cr}^{6+}$  and  $\text{Cr}^{3+}$ ), RS ( $\text{Cr}^{6+}$ ), and ESR ( $\text{Cr}^{5+}$ ).<sup>67,150</sup> For example, the DRS and ESR spectra of  $\text{Cr}/\text{Al}_2\text{O}_3$ , mixed with silica and alumina, and  $\text{Cr}/\text{SiO}_2$ , mixed with alumina and mordenite are presented in Figures 18 and 19, respectively. Figure 18 shows that  $\text{Cr}^{5+}$  and  $\text{Cr}^{6+}$  are always present on alumina, independently of the mixed oxide. The situation is different for  $\text{Cr}/\text{SiO}_2$ . After mixing with alumina,  $\text{Cr}^{5+}$  and  $\text{Cr}^{6+}$  are located on alumina, while with mordenite, spectra of Cr characteristic for both supports, are obtained. From such studies it was concluded that  $\text{Cr}^{5+}$  and  $\text{Cr}^{6+}$  ions migrate from silica to alumina and to a lesser extent to zeolites. Little migration of  $\text{Cr}^{5+}/\text{Cr}^{6+}$  from alumina to zeolites and

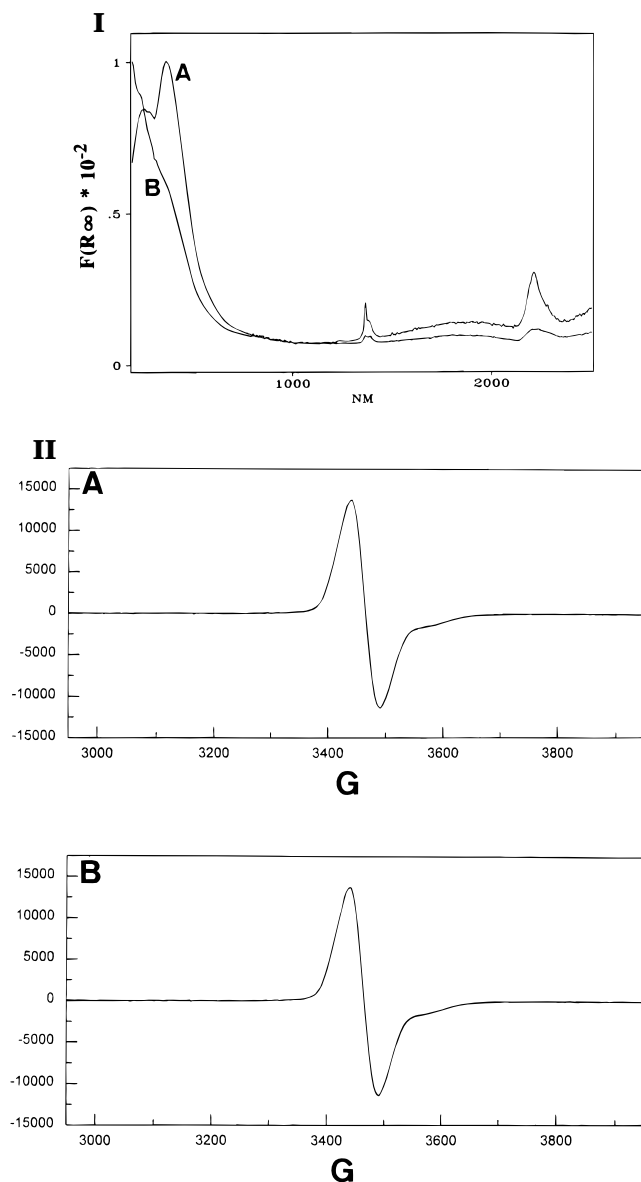


**Figure 18.** Spectroscopic evidence for mobility of Cr species on oxidic surfaces: (I) DRS and (II) ESR spectra of calcined  $\text{Cr}/\text{Al}_2\text{O}_3$ , mixed with alumina (A) and silica (B).

*vice versa* is observed. The latter is indicative of the formation of stable coordination complexes on alumina and zeolites.

In summary, the following preference sequences are obtained for  $\text{Cr}^{3+}$ , alumina  $\approx$  molecular sieve  $\gg$  silica; and for  $\text{Cr}^{6+}$ , alumina  $\gg$  molecular sieve  $\approx$  silica.

## B. Surface Reactivity of Supported Cr

Supported Cr ions show reactivity toward various molecules, as outlined in Figure 20. Three types of interaction can take place: (1) redox reactions, (2) coordinative adsorption, and (3) hydrolysis/condensation reactions.

Reduction/oxidation and hydrolysis/condensation reactions happen when anchored  $\text{Cr}^{6+}$  ions are exposed to several molecules. DRS measurements on calcined  $\text{Cr}/\text{SiO}_2$  and  $\text{Cr}/\text{Al}_2\text{O}_3$  materials show that interaction with (weak) acids, like ethanol and propanol, results in hydrolysis and reduction, while (weak) bases give only reduction.<sup>58</sup> With ethylene, CO and  $\text{H}_2$ ,  $\text{Cr}^{2+}$  is the dominant species on silica,

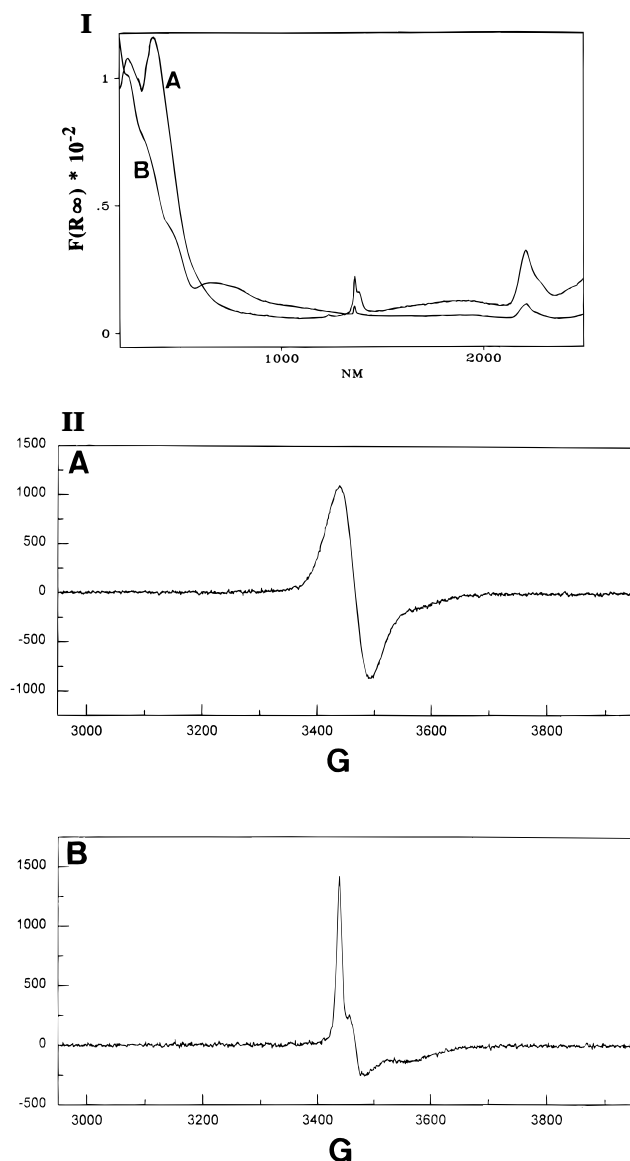


**Figure 19.** Spectroscopic evidence for mobility of Cr species on oxidic surfaces: (I) DRS and (II) ESR spectra of calcined  $\text{Cr}/\text{SiO}_2$ , mixed with alumina (A) and mordenite (B).

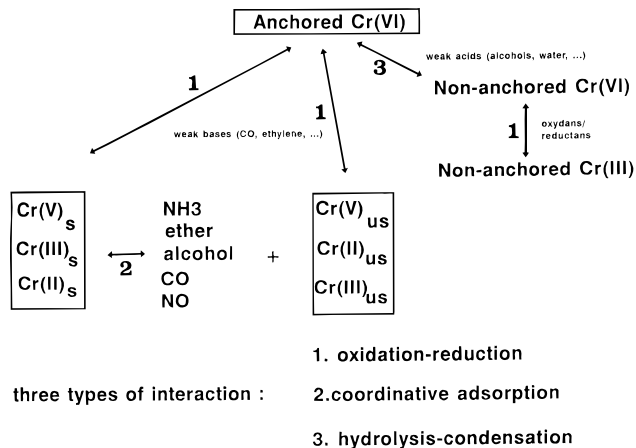


**Figure 20.** Overview of the surface reactivity and the different types of interaction between organic and inorganic molecules and supported Cr.

while on alumina  $\text{Cr}^{3+}$  is preferentially formed.<sup>58</sup> The obtained reduced  $\text{Cr}^{n+}$  species (with  $n = 2, 3$ , or  $5$ ) can be either saturated or unsaturated, and the latter will readily chemisorb different molecules, like am-

monia, water, olefins, alcohols, ethers, CO, and NO.<sup>69-72,151-155,52,35,41,113</sup> The interaction between Cr<sup>5+</sup> and ammonia, ethylene, and water has been extensively investigated by ESR.<sup>36,41</sup> Upon adsorption of small water doses on Cr/SiO<sub>2</sub>, pseudotetrahedral Cr<sup>5+</sup> (coordination number of 4) is converted to a square-planar Cr<sup>5+</sup> (coordination number of 5) and octahedral Cr<sup>5+</sup> (coordination number of 6). The same results are obtained with ethylene instead of water.<sup>41</sup> In the presence of excess water, the chromyl species on silica becomes unstable at elevated temperature, undergoing disproportionation to Cr<sup>3+</sup> and Cr<sup>6+</sup>.<sup>36</sup> On adsorption of ammonia, square-pyramidal Cr<sup>5+</sup> is formed from pseudotetrahedral Cr<sup>5+</sup>. Similar reactions take place on other supports, like alumina, titania, and zirconia.<sup>36</sup> Detailed DRS studies on the interaction between water, alcohol, and ether molecules and silica-supported Cr<sup>2+</sup> ions were carried out by Krauss and co-workers.<sup>52-53,151-155</sup> They show that a coordinative unsaturated Cr<sup>2+</sup> ion can be easily converted to its coordinative saturated counterpart by introducing various molecules. Finally, CO and NO can chemisorb on reduced Cr sites and IR spectroscopy may be used to discriminate between the different coordination geometries, as outlined in the characterization part. In addition, the interaction between supported Cr<sup>2+</sup> and ethylene can be followed by IR spectroscopy. Detailed IR studies were carried out by the group of Zecchina<sup>70-72,75-76,85,133-134</sup> and by Rebenstorf and co-workers.<sup>79-83</sup> Finally, oxygen causes reoxidation of reduced Cr to Cr<sup>6+</sup> with a bright chemiluminescence.<sup>11,158</sup> The intensity of this yellow-orange light flash decreases with increasing reduction temperature of the catalyst, increasing alumina content of the support, and decreasing initial calcination temperature.<sup>106</sup> This chemiluminescence has an orange emission line at 615.8 nm and is due to oxygen atoms (O\*), which are formed on coordinatively unsaturated Cr<sup>2+</sup> sites.<sup>106</sup>

In conclusion, supported Cr ions are very reactive and readily interact with various organic and inorganic molecules. These properties make such materials excellent catalysts for oxidation, hydrogenation-dehydrogenation, and polymerization reactions.

## VII. Catalysis of Cr on Oxidic Surfaces

### A. Oxidation Reactions

The oxidation of organic compounds is a key reaction in inorganic synthesis and traditionally such reactions were performed with stoichiometric amounts of hexavalent chromium salts.<sup>159</sup> However, the Cr<sup>6+</sup> oxidant is usually not regenerated and the associated high costs and toxic effluents result in serious drawbacks, especially on an industrial scale. Consequently, because of the ease of regeneration and recycling of heterogeneous catalysts, much attention has been focused in the last decade on the use of heterogeneous chromium catalysts in oxidation reactions. Furthermore, these catalysts are investigated for the catalytic removal of nitrogen oxide, carbon monoxide, and chlorinated hydrocarbons from exhaust gases.

Supported chromium catalysts have been used for the oxidation of benzophenone<sup>22</sup> (Cr/Al<sub>2</sub>O<sub>3</sub>), diphe-

nylmethane<sup>22</sup> (Cr/Al<sub>2</sub>O<sub>3</sub>), ethanol<sup>160</sup> (Cr/SiO<sub>2</sub>), and methanol.<sup>61,62,67</sup> The oxidation of methanol to formaldehyde was systematically investigated over a series of supported chromium oxide catalysts differing in support composition.<sup>61,62</sup> The surface chromium oxide species were found to be active for methanol oxidation, while the crystalline Cr<sub>2</sub>O<sub>3</sub> particles were essentially inactive for methanol oxidation.<sup>61</sup> The reactivity of the surface chromium oxide species per Cr site per second, turnover frequency (TOF), on the different oxide supports toward redox products was found to vary by approximately a factor of 10<sup>3</sup>: zirconia (1.3 × 10<sup>0</sup> s<sup>-1</sup>), titania (3 × 10<sup>-1</sup> s<sup>-1</sup>), silica (1.6 × 10<sup>-1</sup> s<sup>-1</sup>), niobia (5.8 × 10<sup>-2</sup> s<sup>-1</sup>), and alumina (1.6 × 10<sup>-3</sup> s<sup>-1</sup>). The characterization studies revealed that the same surface chromium oxide species are present on the zirconia, niobia, titania, and alumina supports, and thus, these differences in TOF were not associated with structural changes of the surface chromium oxide species. In addition, changing the ratio of the surface chromate to polychromate species by incorporation of surface titania to silica also did not alter the TOF.<sup>67</sup> The dramatic change in the methanol oxidation TOF is due to the influence of the oxide support ligands which regulate the redox properties of the surface chromium oxide species. It has been proposed that this difference in reactivity is associated with the bridging Cr-O-support bond and generally reflects the reducibility of the oxide support.<sup>62</sup> The selectivity toward formaldehyde during methanol oxidation was dependent on the specific oxide support and surface coverage of the Cr species. Supports possessing strong Lewis acid surface sites, alumina > niobia, were responsible for the formation of significant quantities of the byproduct dimethyl ether. Supports possessing weak Lewis acid surface sites or redox surface sites, zirconia > titania > silica, were responsible for the formation of significant quantities of the byproduct methyl formate. The formation of byproducts by the oxide supports could be reduced by increasing the surface coverage of the Cr species. In the case of Cr/SiO<sub>2</sub>, methyl formate formation could be suppressed by reducing the surface concentration of hydroxyls via high-temperature calcination since these sites were required for the adsorption of methanol and its subsequent reaction with Cr-generated formaldehyde to form methylformate.<sup>60</sup> A formaldehyde selectivity of approximately 90% could be obtained with Cr/SiO<sub>2</sub> catalysts that had been precalcined at 700 °C.<sup>61</sup>

Calcined chromium aluminophosphate molecular sieves (CrAPO-5) are active in the selective oxidation of various secondary alcohols (cyclohexanol, ethylbenzyl alcohol, methylbenzyl alcohol, tetralol, and indanol), using either molecular oxygen or *tert*-butyl hydroperoxide as oxidant. Recently, Chen and Sheldon have shown that a CrAPO-5 material acts as a heterogeneous recyclable catalyst for the liquid-phase autoxidation of cyclohexane to cyclohexanone.<sup>124</sup> Similarly, tetralin and indan were selectively oxidized to 1-tetralone and 1-indanone, respectively. In all these reactions Cr<sup>6+</sup>, as anchored chromate, is proposed as the active oxidation state and the autoxidation mechanism involves an initial free radical autoxidation of the hydrocarbons followed by a selective CrAPO-5-catalyzed intramolecular, heterolytic decomposition

of the secondary alkyl hydroperoxide intermediate to the corresponding ketone and water. Recently, Wang *et al.* found that calcined Cr/MgO materials catalyze the synthesis of 2,6-dimethylphenol from methanol and cyclohexanol at atmospheric pressure.<sup>161</sup>

The selective catalytic reduction (SCR) of NO<sub>x</sub> with NH<sub>3</sub> is the most commonly used method for controlling emissions of oxides of nitrogen from power stations and various materials have been examined for their catalytic performances. The most intensively studied catalysts are based on V/TiO<sub>2</sub>, while supported chromium catalysts have received less attention. Nhyama *et al.* have studied the catalytic activities of various Cr/Al<sub>2</sub>O<sub>3</sub> catalysts.<sup>26–28</sup> The significant N<sub>2</sub>O production, however, above 197 °C made these catalysts unsuitable for technical applications. Amorphous chromia are also effective to reduce NO selectively to N<sub>2</sub>, whereas with crystalline chromia (α-Cr<sub>2</sub>O<sub>3</sub>) formation of N<sub>2</sub> and N<sub>2</sub>O occurred together with significant NH<sub>3</sub> oxidation, the latter especially at higher temperatures.<sup>24,162</sup> Recently, a series of titania-supported chromium catalysts were investigated and were found to be active in SCR reactions below 197 K.<sup>25</sup> The NO conversion rate was proportional to the chromia loading up to 5 wt %. Higher loadings resulted in a less efficient use of the chromia species. However, in general, these Cr/TiO<sub>2</sub> catalysts exhibited a TOF that was approximately a factor of 2 lower than comparable V/TiO<sub>2</sub> catalysts which are employed industrially for this reaction. The selectivity toward N<sub>2</sub> production was approximately 80% for the Cr/TiO<sub>2</sub> catalysts and is approximately 100% for the corresponding V/TiO<sub>2</sub> catalysts under the same reaction conditions. The N<sub>2</sub> selectivity exceeded 90% when the catalysts received a hydrogen pretreatment at 447 °C. Thus, the Cr/TiO<sub>2</sub> catalysts are active for the SCR reaction, but are not as selective as the industrial V/TiO<sub>2</sub>.

Heterogeneous chromium catalysts are also active in the oxidation of hydrocarbons. The performances of Cr zeolites in this type of reactions has been reviewed by Tagiev and Minachev.<sup>163</sup> In a recent study, Cr/SiO<sub>2</sub> catalysts were compared with V/SiO<sub>2</sub> and Mo/SiO<sub>2</sub> systems for the oxidation of methane.<sup>164</sup> The Cr/SiO<sub>2</sub> catalyst was found to be the most active catalyst for methane oxidation (Cr > V > Mo). However, the oxidation of methane over the Cr/SiO<sub>2</sub> catalyst resulted in complete combustion of methane, whereas the V/SiO<sub>2</sub> and Mo/SiO<sub>2</sub> catalysts yielded significant amounts of formaldehyde. In addition, heterogeneous chromium catalysts are active in the oxidation of chlorinated hydrocarbons, like methylene chloride.<sup>19–20</sup> Chatterjee and Greene have compared H-Y, Ce-Y, and Cr-Y molecular sieves for the vapor-phase oxidation of CH<sub>2</sub>Cl<sub>2</sub> in excess air between 300 and 500 °C.<sup>19</sup> The conversions varied from 17 to 99% and the catalytic activity decreases in the order: Cr-Y > H-Y > Ce-Y, while the selectivity among the catalysts was quite similar, with HCl and CO being the major products. In another paper, the same group compared Co-Y, Cr-Y, and Mn-Y catalysts for the catalytic oxidation of methylene chloride, trichloroethylene, and carbon tetrachloride.<sup>20</sup> They show, however, that Co-Y was superior to the Cr-Y catalyst.

## B. Hydrogenation–Dehydrogenation Reactions

Supported chromium oxide catalysts are extensively studied for hydrogenation and dehydrogenation reactions. The catalytic dehydrogenation of light alkanes is especially of great industrial importance because it represents a route to obtain alkenes from feedstocks of low-cost saturated hydrocarbons.<sup>15</sup>

The catalytic performances of Cr/Al<sub>2</sub>O<sub>3</sub> catalysts in alkane dehydrogenation was discovered by Frey and Huppke in 1933<sup>165–166</sup> and is generally known as the Houdry catalyst.<sup>167</sup> This catalyst catalyzes the conversion of e.g. propane to propene, butane to butadiene, and ethylbenzene to styrene at relatively high temperature (450–700 °C) and low pressure (1–5 bar). Because of the different side reactions (cracking and coking), due to the alumina support, the catalyst is easily deactivated and, consequently, regeneration is required. Multiple catalyst beds permit dehydrogenation to take place continuously and typical Cr loadings are above 5 wt %. Details about the surface chemistry of these materials can be found in the review of Poole and MacIver.<sup>168</sup> Recently, the group of Indovina has studied the activity of Cr/ZrO<sub>2</sub> catalysts in the dehydrogenation of propane.<sup>15</sup> They have shown that mononuclear Cr<sup>3+</sup> species are the active centers, whereas surface oxygens adjacent to this Cr<sup>3+</sup> ion are most probably involved in the dehydrogenation site.

The same type of catalysts can be used for hydrogenation reactions, but due to thermodynamical reasons, these reactions require low temperature and relatively high pressures. Important contributions in this field were made in the 1960s by Selwood<sup>169–171</sup> and Burwell *et al.*<sup>172–180</sup> These authors investigated the catalytic properties of pure Cr<sub>2</sub>O<sub>3</sub>, Cr/Al<sub>2</sub>O<sub>3</sub>, and Cr/SiO<sub>2</sub>. Burwell and co-workers discussed in a series of papers the properties of a chromium oxide gel in the hydrogenation of various olefins. In addition, isotopic exchange experiments, the addition of deuterium to olefins, and the elucidation of the stereochemistry of the hydrogenation reactions are presented. From his work Burwell proposed a model for the mechanism of the reaction.<sup>172–180</sup> The site was supposed to consist of a Cr<sup>3+</sup> cation and an oxygen anion, the Cr<sup>3+</sup> cation being accessible from the gas phase because it was situated next to a surface anion vacancy. Hydrogen was assumed to become adsorbed by heterolytical fission with the hydride ion becoming connected to the cation in the surface anion vacancy and the proton being bonded by oxygen. The olefin subsequently formed a carbanion by reaction with the hydride ion, and the final reaction is the combination of the carbanion and the proton to form the paraffin. Cr/Al<sub>2</sub>O<sub>3</sub>, Cr/SiO<sub>2</sub>, and Cr/MgO have also been studied by other authors for the hydrogenation of propene and H<sub>2</sub>–D<sub>2</sub> equilibration.<sup>14,16,181–183</sup> Selwood<sup>184</sup> suggested that Cr<sup>3+</sup> ions are the active sites for catalytic hydrogen–deuterium equilibration over α-Cr<sub>2</sub>O<sub>3</sub>, whereas Indovina *et al.* have shown that the activity of Cr/SiO<sub>2</sub> catalysts is linked to the presence of Cr<sup>2+</sup> ions.<sup>170</sup> However, Wittgen *et al.* have shown that exhaustively reduced Cr/SiO<sub>2</sub> catalysts, which contain predominantly Cr<sup>2+</sup>, are inactive and Cr<sup>3+</sup> is proposed as the active site.<sup>14,16</sup> More recently, Indovina and co-workers have studied the performances of Cr/ZrO<sub>2</sub> catalysts in propene hydrogenation as a

function of the reduction treatment.<sup>185–186</sup> The catalytic activity increases when the average oxidation state of Cr decreases from 5.5 to about 3. Furthermore, reduced Cr/ZrO<sub>2</sub> catalysts were 3.6 to 100 times more active than Cr/SiO<sub>2</sub> and Cr/Al<sub>2</sub>O<sub>3</sub> catalysts, and mononuclear Cr<sup>3+</sup>, formed from the reduction of isolated Cr<sup>5+</sup>, is proposed as the active center.

In summary, hydrogenation and dehydrogenation reactions can be conducted over supported chromium catalysts, but active catalysts can only be obtained after some pretreatment, an evacuation or a passage of an inert gas over the catalyst at high temperature, which is probably connected with the necessity to create surface anion vacancies. Cr/Al<sub>2</sub>O<sub>3</sub> catalysts are industrially important in dehydrogenation reactions.

### C. Polymerization Reactions

Cr/SiO<sub>2</sub> catalysts have been intensively studied for polymerization reactions since Hogan and Banks discovered in 1951 that these systems catalyze the polymerization of olefins.<sup>10,187</sup> Hogan and Banks were trying to make gasoline components from propylene with a new catalyst and found, rather accidentally, that white powder kept plugging their reactor beds. Since then, the processes based on the Phillips catalyst, named after the company name of the inventors, have been successfully commercialized and most of the high-density polyethylene (HDPE) probably comes from this type of catalysts. Furthermore, the use has been extended to the production of linear low-density polyethylene (LLDPE), which is obtained by ethylene copolymerization in the presence of small quantities of  $\alpha$ -olefins (1-butene, 1-hexene, and 1-octene). Actually a whole battery of chromium-based catalysts are now used in the Phillips polymerization process, and each catalyst produces its own polymer type with typical properties, acquired by the customers. Details about reactor design and characteristics of the produced polymers can be found in reviews of Hogan<sup>13</sup> and McDaniel.<sup>6,188</sup>

Prior to use in ethylene polymerization, the Cr/SiO<sub>2</sub> catalysts need to be activated at high temperatures to remove adsorbed water and to reduce the surface hydroxyl population since both retard the ethylene polymerization reaction. During activation, Cr is anchored on the surface by reaction with the hydroxyl groups of the support and typical surface chromium species are formed. Upon exposure to the reducing ethylene stream, these surface chromium species becomes reduced and formaldehyde is formed as the oxidation product.<sup>189</sup> The induction time observed in ethylene polymerization is caused by this first reaction and the displacement of the oxidation products. However, ethylene polymerization occurs immediately with catalysts prerduced with CO or an alkylaluminum compound. The second reaction is then the alkylation in which the first polymer chain starts growing and very little is known about this step.<sup>188</sup>

The two subsequent reaction steps, occurring continuously and simultaneously during polyethylene polymerization, are propagation and chain transfer. During propagation, ethylene is inserted into a Cr-alkyl bond extending the polymer chain with one unit, while by  $\beta$ -H elimination the chain is cleaved

and a new one may begin on the same Cr site. The time needed to grow a chain is typically less than a second and the chain length is determined by the rate of propagation relative to elimination, and both are extremely sensitive to the local environment around the active Cr center. Therefore, different Cr sites may make different chain lengths.

Since the discovery of the Phillips polymerization catalysts, a lively debate has been started about the active site for olefin polymerization and every oxidation state between +6 and +2 has been proposed.<sup>6</sup> However, the main species after reduction with CO and ethylene is Cr<sup>2+</sup>, which readily coordinate and polymerize ethylene. The ability of the Cr/SiO<sub>2</sub> catalysts to be mainly reduced to Cr<sup>2+</sup>, may be one of the reasons that this catalyst is so superior to other catalysts such as Cr/Al<sub>2</sub>O<sub>3</sub>, which can only be reduced to Cr<sup>3+</sup>. Hopefully, this issue can be resolved in the future with *in situ* quantitative spectroscopical investigations.

The efficiency of the supported chromium catalysts decreases with increasing Cr loading. Typical Cr loadings in Phillips catalysts are 1 wt % for slurry type and 0.2 wt % for gas-phase polymerization.<sup>187</sup> Lower polymer weights are obtained by increasing the catalyst activation temperature and by using silicas having larger pore diameters. Furthermore, industrial Cr/SiO<sub>2</sub> catalysts are sometimes promoted by the addition of surface titania to the catalyst. The addition of the surface titania enhances the polymerization rate and alters the molecular weight distribution of the polyethylene product.<sup>196–199</sup> The above-described characterization studies revealed that the addition of surface titania to pyrogenic Cr/SiO<sub>2</sub> changes the predominant surface monochromate species to comparable amounts of surface monochromate and polychromate species by associating the surface Cr species with the surface titania sites. The coordination of the surface Cr species with the surface titania sites on the silica support, via formation of Cr–O–Ti bonds,<sup>196</sup> may account for the enhanced activity of such catalysts and the presence of two distinct active sites may give rise to a different product distribution observed with Cr/Ti/SiO<sub>2</sub> catalysts

Finally, zeolites loaded with Cr ions have been found to be also active in ethylene polymerization.<sup>114,200–201</sup> Yashima *et al.* found that Cr<sup>3+</sup>-exchanged zeolite Y was active in ethylene polymerization only when it was activated *in vacuo*, and was completely inactive after its oxidation by oxygen or reduction by CO or H<sub>2</sub>.<sup>114</sup> However, there is presently no consensus about the active Cr site. According to Wichterlova and co-workers, a necessary condition for ethylene polymerization is the presence of a vacant coordination sphere in an isolated Cr ion and its localization in an accessible zeolitic site.<sup>201</sup>

### VIII. Concluding Remarks

Chromium ions on surfaces of inorganic oxides possess a wide variability in oxidation state, coordination numbers and molecular structure. This variability forms the basis for their diverse chemical behavior, especially important in the field of environmental chemistry and heterogeneous catalysis. In this review paper we have shown that:

(1) The surface chemistry of chromium can be elucidated by making use of a multitechnique approach in which different complementary characterization techniques are applied on the same set of materials and in which advanced mathematical tools are introduced.

(2) There exists an intimate relationship between the surface chemistry of chromium and the structure/composition of inorganic oxides.

(3) The chemical properties of supported Cr ions make such materials excellent catalysts for oxidation, hydrogenation–dehydrogenation, and polymerization reactions.

The general picture of the surface chemistry of supported Cr is as follows:

(1) Under hydrated conditions, the chemistry of Cr at the surface is determined by the isoelectric point, the surface area of the support, and the Cr loading. Thus, at low loadings and high surface areas, the monochromate:dichromate ratio increases with increasing isoelectric point of the support. A tendency toward the formation of polychromates is observed for higher loadings and lower surface areas. After calcination, chromium oxides are anchored onto the surface by reactions with the hydroxyl groups and their molecular structure is determined by the composition and type of the support, the Cr loading, and the treatment.

(2) Under reducing conditions, Cr<sup>5+</sup>, Cr<sup>3+</sup>, and Cr<sup>2+</sup> are present, each under different coordination and polymerization degrees, depending on the support type and composition. In particular, reduction to Cr<sup>3+</sup> for supported Cr on alumina and to Cr<sup>2+</sup> for supported Cr on silica, which parallels the hardness/softness character of these supports.

(3) Supported Cr ions are mobile and possess a high reactivity toward various molecules, like alcohols, ethylene, carbon monoxide, and water. In general, the redox behavior is support type- and composition-dependent and supported Cr ions are easier to reduce on chemically softer supports. Thus, the oxide support acts as a ligand that controls the redox properties of the supported Cr ions.

(4) The chemistry of Cr on amorphous surfaces or on the surfaces of molecular sieves is quite similar.

In conclusion, chromium ions supported on inorganic oxides are complex systems and their characterization requires a battery of complementary techniques. A detailed quantitative picture at the molecular level is obtained by using advanced mathematical and experimental tools. It is also clear that ultimately, spectroscopic techniques have to be developed which allow measurements in conditions as closely as possible to “real conditions” of e.g. a catalytic experiment. Thus, extension to *in situ* spectroscopic investigations of Cr supported systems is the logical next step, which will allow the development of useful structure–activity relationships for predictions in the field of environmental control and heterogeneous catalysis.<sup>202–203</sup>

## IX. List of Abbreviations

DRS	diffuse reflectance spectroscopy
DTA	differential thermal analysis
ESR	electron spin resonance
EXAFS	extended X-ray absorption fine structure

IEP	isoelectric point
IR	infrared spectroscopy
ISS	ion-scattering spectroscopy
MS	molecular sieve
RS	Raman spectroscopy
SEM	scanning electron microscopy
SIMS	secondary ion mass spectrometry
SQUID	superconducting quantum interference devices
TPO	temperature-programmed oxidation
TPR	temperature-programmed reduction
XANES	X-ray absorption near-edge structure
XPS	X-ray photoelectron spectroscopy
XRD	X-ray diffraction

## X. Acknowledgments

B.M.W. acknowledges the N.F.W.O. (Nationaal Fonds voor Wetenschappelijk Onderzoek) for a position as postdoctoral research fellow. This work was financially supported in the frame of the FKFO (Fonds voor Kollektief Fundamenteel Onderzoek) and the GOA (Geconcerteerde Onderzoeksactie) of the Flemish Government. This paper is dedicated to the engineering students at K.U. Leuven who have contributed to advancing the surface chemistry of chromium in inorganic oxides (Leo De Ridder, Hans Spooren, An Verberckmoes, An Buttiens, Bart Schoofs, and Alexander De Baets).

## XI. References

- (1) Greenwood, N. N.; Earnshaw, A. *Chemistry of the Elements*; Pergamon Press: Oxford, 1984.
- (2) Gerhartz, W. *Ullmann's Encyclopedia of Industrial Chemistry*; Weinheim: 1986.
- (3) Stumm, W.; Morgan, J. J. *Aquatic Chemistry, An introduction emphasizing chemical equilibria in natural waters* 2nd ed.; John Wiley & Sons: New York, 1981.
- (4) Stumm, W. *Aquatic Surface Chemistry, Chemical processes at the particle-water interface*; John Wiley & Sons: New York, 1987.
- (5) Richard, F. C.; Bourg, A. C. M. *Water Res.* **1991**, *25*, 807.
- (6) McDaniel, M. P. *Adv. Catal.* **1986**, *33*, 4.
- (7) Burns, R. M. *Mineralogical applications of crystal field theory*, 2nd ed.; Cambridge University Press: Cambridge, 1993.
- (8) Fendorf, S. E.; Fendorf, M.; Sparks, D. L.; Gronsky, R. *J. Colloids Interface Sci.* **1992**, *153*, 37.
- (9) Fendorf, S. E.; Lamb, G. M.; Stapleton, M. G.; Kelley, M. J.; Sparks, D. L. *Environ. Sci. Technol.* **1994**, *28*, 284.
- (10) Hogan, J. P.; Banks, R. L. Belg. Pat. 530617, 1955.
- (11) Hogan, J. P. *J. Polym. Sci.* **1970**, *8*, 2637.
- (12) Hogan, J. P.; Norwood, D. D.; Ayres, C. A. *J. Appl. Polym. Sci.* **1981**, *36*, 49.
- (13) Hogan, J. P. *Appl. Catal. Technol.* Leach, B. E., Ed.; Academic Press: New York, 1983; Vol. 1, p 149.
- (14) Wittgen, P. P. M. M.; Groeneveld, C.; Zwaans, P. J. C. J. M.; Morgenstern, H. J. B.; van Heugten, A. H.; van Heumen, C. J. M.; Schuit, G. C. A. *J. Catal.* **1982**, *77*, 360.
- (15) De Rossi, S.; Ferraris, G.; Fremiotti, S.; Cimino, A.; Indovina, V. *J. Appl. Catal. A: General* **1992**, *81*, 113.
- (16) Groeneveld, C.; Wittgen, P. P. M. M.; van Kersbergen, A. M.; Hestrom, P. L. M.; Nuijten, C. E.; Schuit, G. C. A. *J. Catal.* **1979**, *59*, 153.
- (17) Grunert, W.; Saffert, W.; Feldhaus, R.; Anders, K. *J. Catal.* **1986**, *99*, 149.
- (18) Grunert, W.; Shpiro, E. S.; Feldhaus, R.; Anders, K.; Antoshin, G. V.; Minachev, K. M. *J. Catal.* **1986**, *99*, 149.
- (19) Chatterjee, S.; Greene, H. L. *J. Catal.* **1991**, *130*, 76.
- (20) Chatterjee, S.; Greene, H. L.; Park, J. Y. *J. Catal.* **1992**, *138*, 179.
- (21) Chen, J. D.; Dakka, J.; Neeleman, E.; Sheldon, R. A. *J. Chem. Soc., Chem. Commun.* **1993**, 1379.
- (22) Clark, J. H.; Kybett, A. P.; Landon, P.; Macquarrie, D. J.; Martin, K. *J. Chem. Soc., Chem. Commun.* **1989**, 1355.
- (23) Yamaguchi, T.; Tan-No, M.; Tanabe, K. *Preparation of Catalysts V*; Poncelet, G., et al., Eds.; Elsevier Science Publishers B. V.: Amsterdam, 1991; p 567.
- (24) Duffy, B. L.; Curry-Hyde, H. E.; Cant, N. W.; Nelson, P. F. *J. Phys. Chem.* **1993**, *97*, 1729.
- (25) Engweiler, J.; Nickl, J.; Baiker, A.; Kohler, K.; Schlapfer, C. W.; Zelewsky von, A. *J. Catal.* **1994**, *145*, 141.
- (26) Nhyama, H.; Murata, K.; Can, H. V.; Echigoya, E. *J. Catal.* **1977**, *48*, 194.

- (27) Nhyama, H.; Murata, K.; Can, H. V.; Echigoya, E. *J. Catal.* **1977**, *48*, 201.
- (28) Nhyama, H.; Murata, K.; Can, H. V.; Echigoya, E. *J. Catal.* **1980**, *62*, 1.
- (29) Pourbaix, M. *Atlas of electrochemical equilibria in aqueous solutions*; Pergamon Press: Elmsford, NI, 1966.
- (30) Early, J. E.; Cannon, R. D. *Transition Met. Chem.* **1966**, *1*, 33.
- (31) Rao, C. N. R.; Rao, G. V. S. Transition metal oxides. *Natl. Stand. Ref. Data Ser.* **1964**, NSRDS-NBS49.
- (32) Kung, H. H. *Transition metal oxides: surface chemistry and catalysis. Stud. Surf. Sci. Catal.* **1989**, *45*.
- (33) Burns, R. G. *Mineralogical Applications of Crystal Field Theory*, 2nd ed., Cambridge University Press: Cambridge, 1993.
- (34) O'Reilly, D. E.; MacIver, D. S. *J. Phys. Chem.* **1962**, *66*, 276.
- (35) O'Reilly, D. E.; Santiago, F. D.; Squires, R. G. *J. Phys. Chem.* **1969**, *73*, 3172.
- (36) Cordischi, D.; Campa, M. C.; Indovina, V.; Occhiuzzi, M. *J. Chem. Soc., Faraday Trans.* **1994**, *90* (1), 207.
- (37) Cordischi, D.; Indovina, V.; Occhiuzzi, M. *J. Chem. Soc., Faraday Trans.* **1991**, *87* (20), 3443.
- (38) Cimino, A.; Cordischi, D.; De Rossi, S.; Ferraris, G.; Gazzoli, D.; Indovina, V.; Occhiuzzi, M.; Valigi, M. *J. Catal.* **1991**, *127*, 761.
- (39) Goupil, J. M.; Hemidy, J. F.; Cornet, D. *J. Chim. Phys.* **1976**, *73*, 431.
- (40) Hubald, J. Z. *Chem.* **1977**, *17*, 273.
- (41) Kazanski, V. B.; Turkevich, J. *J. Catal.* **1967**, *8*, 231.
- (42) Przhevalskaya, L. K.; Shvets, V. A.; Kazanskii, V. B. *Kinet. Katal.* **1970**, *11*, 1310.
- (43) Reijen van, L. L.; Cossee, P. *Disc. Faraday Soc.* **1966**, *41*, 277.
- (44) Indovina, V.; Cordischi, D.; De Rossi, S.; Ferraris, G.; Ghiotti, G.; Chiorina, A. *J. Mol. Catal.* **1991**, *68*, 53.
- (45) Kohler, K.; Shlapfer, C. W.; Zelewsky von, A.; Nickl, J.; Engweiler, J.; Baiker, A. *J. Catal.* **1993**, *143*, 201.
- (46) Weckhuysen, B. M.; De Ridder, L. M.; Grobet, P. J.; Schoonheydt, R. A. *J. Phys. Chem.* **1995**, *99*, 320.
- (47) Weckhuysen, B. M.; Schoonheydt, R. A.; Mabbs, F. E.; Collison, D. *J. Chem. Soc., Faraday Trans.* **1996**, *92*, 2431.
- (48) Zecchina, A.; Garrone, E.; Ghiotti, G.; Morterra, C.; Borello, E. *J. Phys. Chem.* **1975**, *79*, 966.
- (49) Fouad, N. E.; Knozinger, H.; Zaki, M. I.; Mansour, S. A. A. *Z. Phys. Chem.* **1991**, *171*, 75.
- (50) Fubini, B.; Ghiotti, G.; Stradella, L.; Garrone, E.; Morterra, C. *J. Catal.* **1980**, *66*, 200.
- (51) Ghiotti, G.; Garrone, E.; Della Gatta, G.; Fubini, B.; Giamello, E. *J. Catal.* **1983**, *80*, 249.
- (52) Krauss, H. L.; Stach, H. Z. *Anorg. Allg. Chem.* **1975**, *414*, 97.
- (53) Krauss, H. L.; Rebenstorf, B.; Westphal, U. Z. *Anorg. Allg. Chem.* **1975**, *414*, 97.
- (54) Ellison, A.; Oubridge, J. O. V.; Sing, K. S. W. *J. Chem. Soc.* **1970**, *66*, 1004.
- (55) Ellison, A.; Sing, K. S. W. *J. Chem. Soc., Faraday Trans. 1* **1978**, *74*, 2017.
- (56) Weckhuysen, B. M.; De Ridder, L. M.; Schoonheydt, R. A. *J. Phys. Chem.* **1993**, *97*, 4756.
- (57) Weckhuysen, B. M.; Verberckmoes, A. A.; Buttiens, A. L.; Schoonheydt, R. A. *J. Phys. Chem.* **1994**, *98*, 579.
- (58) Weckhuysen, B. M.; Wachs, I. E.; Schoonheydt, R. A. *Stud. Surf. Sci. Catal.* **1995**, *91*, 151.
- (59) Hardcastle, F. D.; Wachs, I. E. *J. Mol. Catal.* **1988**, *46*, 173.
- (60) Ianibello, A.; Marengo, S.; Tittarelli, P.; Morelli, G.; Zecchina, A. *J. Chem. Soc., Faraday Trans. 1* **1984**, *80*, 2209.
- (61) Kim, D. S.; Tatibouet, J. M.; Wachs, I. E. *J. Catal.* **1992**, *136*, 209.
- (62) Kim, D. S.; Wachs, I. E. *J. Catal.* **1993**, *142*, 166.
- (63) Vuurman, M. A.; Stufkens, D. J.; Oskam, A.; Moulijn, J. A.; Kapteijn, F. *J. Mol. Catal.* **1990**, *60*, 83.
- (64) Vuurman, M. A.; Wachs, I. E. *J. Phys. Chem.* **1992**, *96*, 5008.
- (65) Vuurman, M. A.; Wachs, I. E.; Stufkens, D. J.; Oskam, A. *J. Mol. Catal.* **1993**, *80*, 209.
- (66) Vuurman, M. A.; Hardcastle, F. D.; Wachs, I. E. *J. Mol. Catal.* **1993**, *84*, 193.
- (67) Jehng, J. M.; Wachs, I. E.; Weckhuysen, B. M.; Schoonheydt, R. A. *J. Chem. Soc., Faraday Trans.* **1995**, *91*, 953.
- (68) Deo, G.; Wachs, I. E. *J. Phys. Chem.* **1991**, *95*, 5889.
- (69) Zecchina, A.; Garrone, E.; Ghiotti, G.; Morterra, C.; Borello, E. *J. Phys. Chem.* **1975**, *79*, 972.
- (70) Zecchina, A.; Garrone, E.; Ghiotti, G.; Morterra, C.; Borello, E. *J. Phys. Chem.* **1975**, *79*, 978.
- (71) Zecchina, A.; Garrone, E.; Ghiotti, G.; Morterra, C.; Borello, E. *J. Phys. Chem.* **1975**, *79*, 984.
- (72) Zecchina, A.; Spoto, G.; Ghiotti, G.; Garrone, E. *J. Mol. Catal.* **1994**, *86*, 423.
- (73) Zielinski, P. A.; Dalla Lana, I. G. *J. Catal.* **1992**, *137*, 368.
- (74) Zielinski, P. A.; Szymura, J. A.; Dalla Lana, I. G. *Catal. Lett.* **1992**, *13*, 331.
- (75) Ghiotti, G.; Garrone, E.; Zecchina, A. *J. Mol. Catal.* **1988**, *46*, 61.
- (76) Ghiotti, G.; Garrone, E.; Zecchina, A. *J. Mol. Catal.* **1991**, *65*, 73.
- (77) Kim, C. S.; Woo, S. I. *J. Mol. Catal.* **1992**, *73*, 249.
- (78) Nishimura, M.; Thomas, J. M. *Catal. Lett.* **1993**, *19*, 33.
- (79) Rebenstorf, B.; Larsson, R. Z. *Anorg. Allg. Chem.* **1981**, *478*, 119.
- (80) Rebenstorf, B.; Larsson, R. *J. Catal.* **1983**, *84*, 240.
- (81) Rebenstorf, B. *J. Mol. Catal.* **1986**, *38*, 355.
- (82) Rebenstorf, B. *J. Mol. Catal.* **1989**, *56*, 170.
- (83) Rebenstorf, B. *J. Catal.* **1989**, *117*, 71.
- (84) Schram-Marth, M.; Wokaun, A.; Baiker, A. *J. Catal.* **1992**, *138*, 306.
- (85) Spoto, G.; Bordiga, S.; Garrone, E.; Ghiotti, G.; Zecchina, A. *J. Mol. Catal.* **1992**, *74*, 175.
- (86) Best, S. A.; Squires, R. G.; Walton, R. A. *J. Catal.* **1977**, *47*, 292.
- (87) Cimino, A.; De Angelis, B. A.; Luchetti, A.; Minelli, G. *J. Catal.* **1976**, *45*, 316.
- (88) Merryfield, R.; McDaniel, M.; Parks, G. *J. Catal.* **1982**, *77*, 348.
- (89) Gazzoli, D.; Occhiuzzi, M.; Cimino, A.; Minelli, G.; Valigi, M. *Surf. Interface Anal.* **1992**, *18*, 315.
- (90) Hercules, D. M.; Procter, A.; Houalla, M. *Acc. Chem. Res.* **1994**, *27*, 387.
- (91) Cimino, A.; Cordischi, D.; De Rossi, S.; Ferraris, G.; Gazzoli, D.; Indovina, V.; Minelli, G.; Occhiuzzi, M.; Valigi, M. *J. Catal.* **1991**, *127*, 744.
- (92) Parks, G. A. *Chem. Rev.* **1965**, *65*, 177.
- (93) Weckhuysen, B. M.; Schoonheydt, R. A.; Hu, H.; Deo, G.; Wachs, I. E.; Cho, S. J.; Ryou, R.; Kijlstra, S.; Poels, E. *J. Chem. Soc., Faraday Trans.* **1995**, *91*, 3245.
- (94) Weckhuysen, B. M.; Schoonheydt, R. A.; Hu, H.; Deo, G.; Wachs, I. E. *J. Phys. Chem.*, to be published.
- (95) Jehng, J. M.; Turek, A. M.; Wachs, I. E. *Appl. Catal. A: General* **1992**, *83*, 179.
- (96) Turek, A. M.; Wachs, I. E.; DeCanio, E. *J. Phys. Chem.* **1992**, *96*, 5000.
- (97) McDaniel, M. P. *J. Catal.* **1981**, *67*, 71.
- (98) McDaniel, M. P. *J. Catal.* **1982**, *76*, 17.
- (99) McDaniel, M. P. *J. Catal.* **1982**, *76*, 29.
- (100) McDaniel, M. P. *J. Catal.* **1982**, *76*, 37.
- (101) Groeneveld, C.; Wittgen, P. P. M. M.; Kersbergen van, A. M.; Hestrom, P. L. M.; Nuijten, C. E.; Schuit, G. C. A. *J. Catal.* **1979**, *59*, 153.
- (102) Ellison, A. *J. Chem. Soc., Faraday Trans. 1* **1984**, *80*, 2581.
- (103) Spitz, R. *J. Catal.* **1974**, *35*, 345.
- (104) Spitz, R.; Revillon, A.; Guyot, A. *J. Catal.* **1974**, *35*, 335.
- (105) Cordischi, D.; Indovina, V.; Occhiuzzi, M. *Appl. Surf. Sci.* **1992**, *55*, 233.
- (106) Weckhuysen, B. M. Surface Chemistry of Chromium in Inorganic Oxides; PhD. Thesis, Nr. 282 of Faculty of Applied Biological Sciences, K.U. Leuven, 1995.
- (107) Fouad, N. E.; Knozinger, H.; Zaki, M. I. *Z. Phys. Chem.* **1994**, *186*, 231.
- (108) Scierka, S. J.; Houalla, M.; Procter, A.; Hercules, D. M. *J. Phys. Chem.* **1995**, *99*, 1537.
- (109) Fouad, N. E.; Knozinger, H.; Zaki, M. I. *Z. Phys. Chem.* **1994**, *186*, 231.
- (110) Ehrhardt, K.; Richter, M.; Roost, V.; Ohlmann, G. *Appl. Catal.* **1985**, *17*, 23.
- (111) Kellerman, R.; Klier, K. in *Molecular Sieves -II*; Katzer, J. R., Ed.; American Chemical Society: Washington, DC, 1977; p 120.
- (112) Coughlan, B.; McCann, W. A.; Carroll, W. M. *Chem. Ind.* **1977**, 358.
- (113) Pearce, J. R.; Sherwood, D.; Hall, M. B.; Lunsford, J. H. *J. Phys. Chem.* **1980**, *84*, 3215.
- (114) Yashima, T.; Nagata, J.; Shimazaki, Y.; Hara, N. in *Molecular Sieves-II*; Katzer, J. R., Ed.; American Chemical Society: Washington, DC, 1977; p 626.
- (115) Voght, F.; Bremer, H.; Rubinstejn, A. M.; Daservskij, M. I.; Slinkin, A. A.; Kljacko, A. L. *Z. Anorg. Allg. Chem.* **1976**, *423*, 155.
- (116) Kellerman, R.; Hutta, P. J.; Klier, K. *J. Am. Chem. Soc.* **1974**, *96*, 5946.
- (117) Mikheikin, I. D.; Zhidomirov, G. M.; Kazanskii, V. B. *Russ. Chem. Rev.* **1972**, *41* (5), 468.
- (118) Atanasova, V. P.; Shvets, V. A.; Kazanskii, V. B. *Kinet. Katal.* **1977**, *18*, 1033.
- (119) Munuera, G.; Rives, V. In Proceedings of the Vth Ibero-American Symposium on Catalysis, 1978; Vol. 1, p 101.
- (120) Weckhuysen, B. M.; Spooen, H. J.; Schoonheydt, R. A. *Zeolites* **1994**, *14*, 450.
- (121) Naccache, C.; Taarit, Y. B. *J. Chem. Soc., Faraday Trans. 1* **1973**, *69*, 1475.
- (122) Chambellan, A.; Chevreau, T.; Cornet, D. *J. Chim. Phys.* **1978**, *75*, 511.
- (123) Pastore, H. O.; Stein, E.; Davanzo, C. U.; Vichi, E. J. S.; Nakamura, O.; Baesso, M.; Silva, E.; Vargas, H. *J. Chem. Soc., Chem. Commun.* **1990**, 772. Mambirim, J. S. T.; Vichi, E. J. S.; Pastore, H. O.; Davanzo, C. U.; Vargas, H.; Silva, E.; Nakamura, O. *J. Chem. Soc., Chem. Commun.* **1991**, 922.
- (124) Chen, J. D.; Sheldon, R. A. *J. Catal.* **1995**, *153*, 1.
- (125) Weckhuysen, B. M.; Schoonheydt, R. A. *Zeolites* **1994**, *14*, 360.
- (126) Weckhuysen, B. M.; Schoonheydt, R. A. *Stud. Surf. Sci. Catal.* **1994**, *84*, 965.
- (127) Hemidy, J. F.; Cornet, D. *J. Chim. Phys.* **1974**, *5*, 739.
- (128) Hemidy, J. F.; Delavennat, F.; Cornet, D. *J. Chim. Phys.* **1973**, *11-12*, 1716.

- (129) Huang, M.; Deng, Z.; Wang, Q. *Zeolites* **1990**, *10*, 272.
- (130) Nakamura, O.; Mambirim, J. S.; Pastore, H. O.; Vichi, E. J. S.; Gandra, F. G.; Silva, E. C.; Vargas, H.; Pelzi, J. *J. Chem. Soc., Faraday Trans.* **1992**, *88*, 2071.
- (131) Chapus, T.; Tuel, A.; Ben Taarit, Y.; Naccache, C. *Zeolites* **1994**, *14*, 349.
- (132) Kucherov, A. V.; Slinkin, A. A. *J. Mol. Catal.* **1994**, *90*, 323.
- (133) Spoto, G.; Bordiga, S.; Garrone, E.; Ghiotti, G.; Zecchina, A. *J. Mol. Catal.* **1992**, *74*, 175.
- (134) Zecchina, A.; Spoto, G.; Ghiotti, G.; Garrone, E. *J. Mol. Catal.* **1994**, *86*, 423.
- (135) Beran, S.; Jiru, P.; Wichterlova, B. *J. Chem. Soc., Faraday Trans.* **1983**, *79*, 1585.
- (136) Wichterlova, B.; Tvaruzkova, Z.; Novakova, J. *J. Chem. Soc., Faraday Trans.* **1983**, *79*, 1573.
- (137) Helliwel, M.; Kaucic, V.; Cheetham, G. M. T.; Harding, M. M.; Kariuki, B. M.; Rizkallah, P. *Acta Crystallogr. B* **1993**, *49*, 413.
- (138) Belussi, G.; Rigutto, M. S. *Stud. Surf. Sci. Catal.* **1994**, *85*, 177.
- (139) Demuth, D.; Unger, K. K.; Schuth, F.; Srdanov, V. I.; Stucky, G. D. *J. Phys. Chem.* **1995**, *99*, 479.
- (140) Carnaro, U.; Jiru, P.; Tvaruzkova, Z.; Habersberger, K. In *Zeolite Chemistry and Catalysis*; Jacobs, P. A., Eds.; Elsevier Science Publishers, B. V.: Amsterdam, 1991; p 165.
- (141) Vander Puil, N.; Widyawattii, Jansen, J. C.; van Bekkum, H. *Stud. Surf. Sci. Catal.* **1994**, *84*, 211.
- (142) Klotz, M. R. US Pat. 4,299,808, 1981.
- (143) Flanigen, E. M.; Lok, B. M. T.; Patton, R. L.; Wilson, S. T. US Pat. 4,759,919, 1988.
- (144) Mosser, C.; Petit, S.; Mestdagh, M. *Clay Minerol.* **1993**, *28*, 353.
- (145) Gaitte, J. M.; Mosser, C. *J. Phys.: Condens. Matter* **1993**, *5*, 4929.
- (146) Pearson, R. G. *J. Am. Chem. Soc.* **1963**, *85*, 3533.
- (147) Weckhuysen, B. M.; Toufar, H.; DeBaets, A.; Janssen, G. O. A.; Mortier, W. J.; Schoonheydt, R. A. *J. Phys. Chem.*, to be published.
- (148) Weckhuysen, B. M.; Verberckmoes, A. A.; DeBaets, A.; Schoonheydt, R. A. *J. Catal.*, in press.
- (149) Yang, S. J.; Chen, Y. W.; Li, C. *Appl. Catal. A* **1994**, *115*, 59.
- (150) Weckhuysen, B. M.; Schoofs, B.; Schoonheydt, R. A. *J. Chem. Soc., Faraday Trans.* submitted for publication.
- (151) Krauss, H. L.; Naumann, D. *Z. Anorg. Allg. Chem.* **1978**, *446*, 23.
- (152) Hierl, G.; Krauss, H. L. *Z. Anorg. Allg. Chem.* **1973**, *401*, 263.
- (153) Krauss, H. L.; Weissner, B. *Z. Anorg. Allg. Chem.* **1975**, *412*, 82.
- (154) Krauss, H. L.; Stach, H. *Z. Anorg. Allg. Chem.* **1969**, *366*, 34.
- (155) Krauss, H. L. *J. Mol. Catal.* **1988**, *46*, 97.
- (156) Rebenstorf, B.; Sheng, T. C. *Langmuir* **1991**, *10*, 2161.
- (157) Rebenstorf, B.; Anderson, S. L. *J. Chem. Soc., Faraday Trans.* **1990**, *86*, 2783.
- (158) Morys, P.; Gorges, U.; Krauss, H. L. *Z. Naturforsch., B: Anorg. Chem., Org. Chem.* **1984**, *39B*, 458.
- (159) Cainelli, G.; Cardillo, G. *Chromium oxidations in Organic Chemistry*; Springer-Verlag: Berlin, 1984.
- (160) Parllitz, B.; Hanke, W.; Fricke, R.; Richter, M.; Roost, V.; Ohlmann, G. *J. Catal.* **1985**, *94*, 24.
- (161) Wang, F. L.; Tsai, T. F.; Tsai, Y. K.; Cheng, Y. K. *Appl. Catal. A: General* **1995**, *126*, L229.
- (162) Duffy, B. L.; Curry-Hyde, H. E.; Cant, N. W.; Nelson, P. F. *Appl. Catal. B: Environmental* **1994**, *5*, 133.
- (163) Tagiev, D. B.; Minachev, K. M. *Usp. Khim.* **1981**, *50*, 1929.
- (164) Sun, Q.; Klier, K. *J. Catal.*, to be published.
- (165) Frey, F. E.; Huppke, W. F. *Ind. Eng. Chem.* **1933**, *25*, 54.
- (166) Frey, F. E.; Huppke, W. F. US Pat. 2,098,959, 1937.
- (167) Kearby, K. K. In *Catalysis, Fundamental Principles*; Emmet, P. H., Ed.; Reinhold Publishing Corporation: New York, 1955; Vol. 3, Chapter 10, p 453.
- (168) Poole, C. P.; MacIver, D. S. *Adv. Catal.* **1967**, *17*, 223.
- (169) Selwood, P. W. *J. Am. Chem. Soc.* **1966**, *88*, 2676.
- (170) Selwood, P. W. *J. Am. Chem. Soc.* **1970**, *92*, 39.
- (171) Selwood, P. W. *J. Catal.* **1968**, *12*, 263.
- (172) Burwell, R. L.; Littlewood, A. B.; Cardew, M.; Pass, G.; Stoddart, C. T. H. *J. Am. Chem. Soc.* **1960**, *82*, 6272.
- (173) Pass, G.; Littlewood, A. B.; Burwell, R. L. *J. Am. Chem. Soc.* **1960**, *82*, 6284.
- (174) Stoddart, C. T. H.; Pass, G.; Burwell, R. L. *J. Am. Chem. Soc.* **1960**, *82*, 6284.
- (175) Littlewood, A. B.; Burwell, R. L. *J. Am. Chem. Soc.* **1960**, *82*, 6287.
- (176) Cardew, M.; Burwell, R. L. *J. Am. Chem. Soc.* **1960**, *82*, 6289.
- (177) Burwell, R. L.; Read, J. F.; Taylor, K. C.; Haller, G. L. *Z. Phys. Chem. N. F.* **1969**, *64*, 18.
- (178) Burwell, R. L.; Loner, C. J. Proc. 3rd Intern. Congr. Catal., Amsterdam, 1964, p 804.
- (179) Burwell, R. L.; Haller, G. L.; Taylor, K. C.; Read, J. F. *Adv. Catal., Relat., Subj.* **1969**, *20*, 1.
- (180) Burwell, R. L. Electrocatalysis on non-metallic surfaces. In *Chemical theory of chemisorption and catalysis on the surfaces of non-metals*; Nat. Bureau of Standards Special Publication 455, Dec. 9–12, 1975; Government Printing Offices: Washington, DC, issued Nov 1976.
- (181) Iwasawa, Y.; Ogasawa, S. *Chem. Lett.* **1980**, 127.
- (182) Iwasawa, Y.; Sasakim, Y.; Ogasawara, S. *J. Chem. Soc., Chem. Commun.* **1981**, 140.
- (183) Iwasawa, Y. *J. Mol. Catal.* **1982**, *17*, 93.
- (184) Indovina, V.; Cimino, A.; Inversi, M. *J. Phys. Chem.* **1978**, *82*, 285.
- (185) Cimino, A.; Cordischi, D.; De Rossi, S.; Ferraris, G.; Gazzoli, D.; Indovina, V.; Valigi, M. *J. Catal.* **1991**, *127*, 777.
- (186) Cimino, A.; Cordischi, D.; De Rossi, S.; Ferraris, G.; Gazzoli, D.; Indovina, V.; Minelli, G.; Occhuzzi, M.; Valigi, M. In Proc. 9th Int. Congr. Catal., Calgary Phillips, M. J., Terran, M., Ed.; 1988; Vol. 3, p 1465.
- (187) Pasquon, I.; Giannini, U. In *Catalysis, Science and Technology*; Anderson, J. R., Boudart, M., Eds.; Springer-Verlag: Berlin, 1984; Vol. 65; Chapter 2, p 66.
- (188) McDaniel, M. P. *Ind. Eng. Chem. Res.* **1988**, *27*, 1559.
- (189) Baker, L. M.; Carrick, W. L. *J. Org. Chem.* **1970**, *35*, 774.
- (190) Ghiotti, G.; Garrone, E.; Coluccia, S.; Morterra, C.; Zecchina, A. *J. Chem. Soc., Chem. Commun.* **1979**, 1032.
- (191) Rebenstorf, B.; Larsson, R. S. *J. Mol. Catal.* **1981**, *11*, 247.
- (192) Kantcheva, M.; Dalla Lana, I. G.; Szymura, J. A. *J. Catal.* **1995**, *154*, 329.
- (193) Vikulov, K.; Spoto, G.; Coluccia, S.; Zecchina, A. *Catal. Lett.* **1992**, *16*, 117.
- (194) Zielinski, P.; Dalla Lana, I. G. *J. Catal.* **1992**, *137*, 368.
- (195) Krauss, H. L. *Proc. Int. Congr. Catal.*, *5th* **1973**, *1*, 207.
- (196) Pullukat, T. J.; Hoff, R. E.; Shida, M. *J. Polym. Sci., Polym. Chem. Educ.* **1980**, *18*, 2857.
- (197) Conway, S. J.; Falconer, J. W.; Rochester, C. H. *J. Chem. Soc., Faraday Trans. 1* **1989**, *85*, 71.
- (198) Conway, S. J.; Falconer, J. W.; Rochester, C. H.; Downs, G. W. *J. Chem. Soc., Faraday Trans. 1* **1989**, *85*, 1841.
- (199) McDaniel, M. P.; Welch, M. B.; Dreiling, M. J. *J. Catal.* **1983**, *82*, 118.
- (200) Wang, J. K.; Komatsu, T.; Namba, S.; Yashima, T.; Uematsu, T. *J. Mol. Catal.* **1986**, *37*, 327.
- (201) Tvaruzkova, Z.; Wichterlova, B. *J. Chem. Soc., Faraday Trans. 1* **1983**, *79*, 1591.
- (202) Weckhuysen, B. M.; Wachs, I. E. *J. Phys. Chem.* **1996**, *100*, 14437.
- (203) Bensalem, A.; Weckhuysen, B. M.; Schoonheydt, R. A. *J. Phys. Chem.*, submitted for publication.

CR9400440

